# A STUDY OF BENDING OF SANDWICH CANTILEVER BEAMS UNDER VARIOUS TYPES OF LOADING

By

R.V.Ananthasubramanian

Submitted to the Faculty of Science and Engineering of the University of Ottawa in partial fulfillment of the requirements for the degree of

MASTER OF APPLIED SCIENCE

in Mechanical Engineering

September, 1970.

A STUDY OF BENDING OF SANDWICH CANTILEVER BEAMS

UNDER VARIOUS TYPES OF LOADING

~~Adviser~~ Sept: 16, 1970

Candidate

ACKNOWLEDGEMENT

I wish to express my deepest sense of gratitude to Dr. S. Mirza, under whose supervision this project was carried out, for his invaluable suggestions, constant encouragement and stimulating discussions.

I am thankful to Dr. A. Feingold for his continued interest in this project and useful criticism.

I am also thankful to the National Research Council of Canada and the Department of Mechanical Engineering, University of Ottawa for the financial support in the form of Research and Teaching Assistantships.

The many courtesies extended by the personnel of the Materials Laboratory, National Research Council of Canada and the Computing Centre, University of Ottawa are highly appreciated.

The assistance rendered by my friends, Mr. C.P. Khulbe and Mr. A.V. Singh, is gratefully acknowledged.

# ABSTRACT

A theoretical soution for the transverse and axial deformations of sandwich cantilever beams, due to various types of loading has been presented here. This is obtained by the use of Finite Element Method. The use of these deflections in the fundamental equations for sandwiches, yields the stress and strain states. The boundary conditions for this problem are derived from the total potential energy by the variational principle.

Results for the transverse deformation under uniform transverse loading are compared with experimental results.

Photoelastic technique has been used for experimental investigations. Method of shear differences is employed to separate the principal stresses. This technique provides the normal stresses in the face sheets and shear stresses in the core.

The basic assumptions involved in the theory of sandwich materials are finally checked against the experimental results.

TABLE OF CONTENTS

## NOMENCLATURE

| | |
|---|---|
| $f$ | Thickness of face sheets |
| $h$ | Thickness of core |
| $b$ | Width of beam |
| $\alpha$ | Length of beam element |
| $w$ | Transverse deformation |
| $u$ | Axial deformation |
| $p_o$ | Intensity of transverse load |
| $a_i$ | Coefficients of x in polynomials for u and w |
| $m_i, n_i$ | Exponents of x in polynomials for u and w |
| $x, y, z$ | Co-ordinate axes of the beam |
| $L$ | Length of the beam |
| $E_f$ | Young's modulus of face material |
| $G_c$ | Shear modulus of core material |
| $U$ | Strain energy of the beam |
| $W$ | Potential energy of applied loads |
| $F_a$ | Axial load at the nodes |
| $F_t$ | Transverse load at the nodes |
| $\{w\}$ | Generalized displacement vector |
| $\{F\}$ | Consistent load vector of beam element |
| $T$ | Transformation matrix |
| SM | Element stiffness matrix |
| SS | Overall stiffness matrix |
| $\{VL\}$ | Load vector for the entire beam |

# I. INTRODUCTION

A sandwich construction is a multi-layer structure made up of alternating sheets of high-strength material with thick layers of low-strength, low-density material in between them. Because of its low weight-to-strength ratio, it is formed with a variety of non structural core materials such as paper and metal honeycombs, foam plastics, cork etc. The sandwich construction has been employed in airplane wings, rotors in modern helicopters and other light-weight structures. Structural sandwiches are made up of thin, strong and stiff facings or skins bonded to a thick, relatively light and weaker core, providing a light-weight combination which is much stronger and stiffer than the face sheets and core, considered individually.

The basic idea behind sandwich construction is much the same as that in an I beam, which is an efficient structural shape. In this case more material is placed in the flanges situated farthest from the neutral axis and relatively less material is left in the connecting web to make the flanges act together and to resist shear and buckling. In a structural sandwich the face sheets replace the flanges and the core takes the place of the web. The difference being that the core is of a different material than that of the facings, and is spread out unlike the narrow web of an I beam. The facings act together to form an efficient stress couple resisting the external bending moment. The core resists the shear stresses set up by the external loads, in addition to stabilizing the facings against wrinkling and buckling.

The advantages of using sandwich construction have long been recognized in the aircraft industry. These advantages include higher strength-to-weight ratios, smooth surfaces, better stability, absence of potential leaks, high load-carrying capacity, increased fatigue life and high sonic fatigue endurance [3]*. Examples of sandwich construction are: wings, fuselage and tailplane skins, pressure bulkheads, spar webs, ribs, floorings etc.

In this thesis an attempt has been made to analyse the behaviour of a sandwich cantilever beam under given types of loading conditions. The Finite Element Method has been used as a numerical tool to carry out this investigation. For the experimental investigation, the photoelastic technique has been used.

The major portion of the literature available on the analysis of sandwich structures concentrates primarily on the refinement of long-standing theories. Examples of such work are found in papers by Reissner [14], Yu [16], and Hoff [8]. Much attention has also been given to the simplification of some of the more refined theories, so that they are directly applicable in the design problems. A fairly detailed summary of it can be found in Plantemas's work [12]. However, in spite of these simplifications, solution of most of these problems requires the use of trigonometric series expansion. An alternative approach used by various authors is to transform the basic differential

* Numbers within square brackets correspond to the reference numbers at the end of the thesis.

equations in terms of finite difference operators.

A new approximate method of analysis, known as finite element method has acquired considerable popularity in the past decade, and has been used to solve many problems of elasticity.

The finite difference method is basically a mathematical approach by which the derivatives in the differential equations and boundary conditions are replaced by difference operators. The finite element method has both mathematical and physical significance. From the mathematical stand-point the finite element method may be considered as the subdivision of a region, over which the solution is sought, into a number of sub-regions or elements. These sub-regions are connected at a finite number of nodal points, and the continuity of the solution function which is assumed for each sub-region, is enforced at each nodal point so that the assumed solution functions for the sub-regions form a sectionally continuous solution function for the whole region. Physically the finite element method may be thought of, as an approximation to a structure by a finite number of elements interconnected at a finite number of nodal points.

Very little literature is available on the study of sandwich structures using the finite element method. Monforton and Schmit [11] have developed an element to study the behavior of sandwich plates and shells using first-order Hermite interpolation polynomials. Maple [10] has developed an element using two and three-dimensional element shapes to solve problems on sandwich plates and shells. The use of triangular and rectangular element shapes has been illustrated in this work. The shape of a typical element used by Maple is shown in Fig.4, p.11.

In this thesis, a linear beam element is chosen to study the bending of a sandwich cantilever beam with isotropic core and face materials under uniformly distributed transverse loading condition. The theoretical deformation pattern has been compared with experimental results. The theoretical study is also extended to the case of combined axial and transverse loading with uniform and linearly varying axial loads.

The above loading conditions are studied with a view to simulate the following situations. The floor of the fuel tank in the fuselage of an aircraft is a typical example of uniform loading of a sandwich strip. In such a case the facings are usually made up of aluminum ( $E=10^7$ psi ) and the approximate dimensions involved are of the order of 0.05" for the face thickness and about 0.8 to 0.9" for the honeycomb core with a shear modulus of the order of 14000 psi. The case of gas turbine blades with ceramic coatings on alloy steel cores corresponds to a sandwich beam loaded with a centrifugal load along the axis and a transverse gas pressure. Admittedly, the ceramic coating which is termed as the face sheet here, behaves as a good heat resisting medium, rather than as a structural member resisting load. Further, the loading due to gas pressure and the geometry of the turbine blade are by no means sufficiently simple to be treated with this approach. The turbine blade, having a complex geometry is therefore idealized by a beam of uniform cross-section and the gas pressure by a uniform transverse loading.

The experimentation in this work has been confined to the case of a sandwich cantilever beam under uniform transverse loading. A special loading rig, much more complex than the one required in the first case, would be needed to apply axial as well as transverse loads. The stress distribution in the vicinity of the fixed end of the beam was evaluated using the photoelastic technique. As the deformations were of the order of 0.01", it was possible to use the polariscope for measuring the transverse deformations at different points along the length of the beam.

Finite Element Method:

Engineering structures can be considered as an assembly of structural elements interconnected at a discrete number of nodal points. Knowledge of force-displacement relations enables us to derive the properties and study the behaviour of the assembled structure.

In an elastic continuum the true number of interconnecting points is infinite. The concept of finite elements overcomes this by assuming the elastic continuum to be made up of elements interconnected only at a finite number of nodal points at which some fictitious forces representing the actual distributed boundary stresses are applied. The finite element method applied in this thesis is characterized by the choice of a displacement function which satisfies conditions of continuity not only between the nodes but also along the interface of two elements. It follows therefore that, the stresses and strains are derived quantities rather than a direct outcome of the finite element solution. Further, the accuracy and convergence of the finite element solution depend on the number of elements chosen to represent the continuum and the correct application of boundary conditions. Since the boundary conditions introduced for the solution of the problem are displacement-boundary conditions, rather than stress-boundary conditions, it is not unusual to end up with solutions which give rise to a small value for moments and stresses at free boundaries.

Clearly, as in any other numerical method, a series of approximations have been introduced. In the first place, it is not always easy to ensure that the chosen displacement function will satisfy the requirements of displacement continuity between adjacent elements. In the second place, by concentrating the equivalent forces at the nodes, equilibrium conditions are satisfied in the overall sense only. Local violations of equilibrium conditions within each element and on its boundaries will usually arise.

The finite element analysis of an elastic continuum may be divided into three basic phases: structural idealization, evaluation of element properties and structural analysis of the element assemblage. As in any method of structural analysis the problem is to satisfy the following three requirements simultaneously:

a. Equilibrium equations,

b. Compatibility,

c. Force-displacement relationship.

The basic operations of a displacement of analysis of any structure are as follows:

1. Evaluation of the stiffness properties of the individual structural elements expressed in any convenient co-ordinate system.

2. Transformation of the element stiffness properties (derived in the form of a matrix) from the local co-ordinate system to the global co-ordinate system of the complete structural assemblage.*

3. Superposition of the individual element stiffnesses contributing to each nodal point to obtain the total assemblage nodal stiffness matrix.

4. Formulation and solution of the equilibrium equations expressing the relationship between the applied nodal forces {VL}and the resulting nodal displacements {w}**

i.e $\{VL\} = [SS]\,\{w\}$

5. Solution of the above equation for the unknown displacement vector {w} by a standard linear equations-solving process.

---

* In this case, the global co-ordinate system is the same as the local or element co-ordinate system.

** The symbol { } denotes a column vector.

## II. BASIC EQUATIONS AND FORMULATION OF THE PROBLEM

In this thesis the finite element method has been used to predict the displacements in the case of an isotropic sandwich cantilever beam under two types of load conditions. Once the displacements at discrete points are determined, the stress state and strain state can be easily established. This technique involves the choice of a suitable displacement function to represent the transverse and axial displacements of the beam. It is assumed that the displacements are small and the transverse deformation is uniform through the thickness of the sandwich. That is, the effect of core compression is completely neglected.

A quintic polynomial in x is chosen to represent the transverse deformation (w) and a cubic in x for the axial deformation (u). Refer to Fig. 1 for the co-ordinate system. Such a choice of displacement functions leads to five degrees of freedom at each of the two nodes of the beam element. These are w, $w_x$, $w_{xx}$, u and $u_x$. The six arbitrary constants $a_1$, $a_2$ etc. which appear in the expression for the displacement function

$$w(x) = a_1 + a_2 x + a_3 x^2 + a_4 x^3 + a_5 x^4 + a_6 x^5 \qquad (2.1)$$

can be expressed in terms of the six generalized displacement co-ordinates $w_1$, $w_{x1}$, $w_{xx1}$, $w_2$, $w_{x2}$, $w_{xx2}$. Here the Arabic numerals used as subscripts denote the position of the node and further the general notations adopted are:

$$w_x = \frac{dw}{dx} \quad , \qquad w_{xx} = \frac{d^2 w}{dx^2}$$

UNIFORMLY LOADED SANDWICH CANTILEVER BEAM

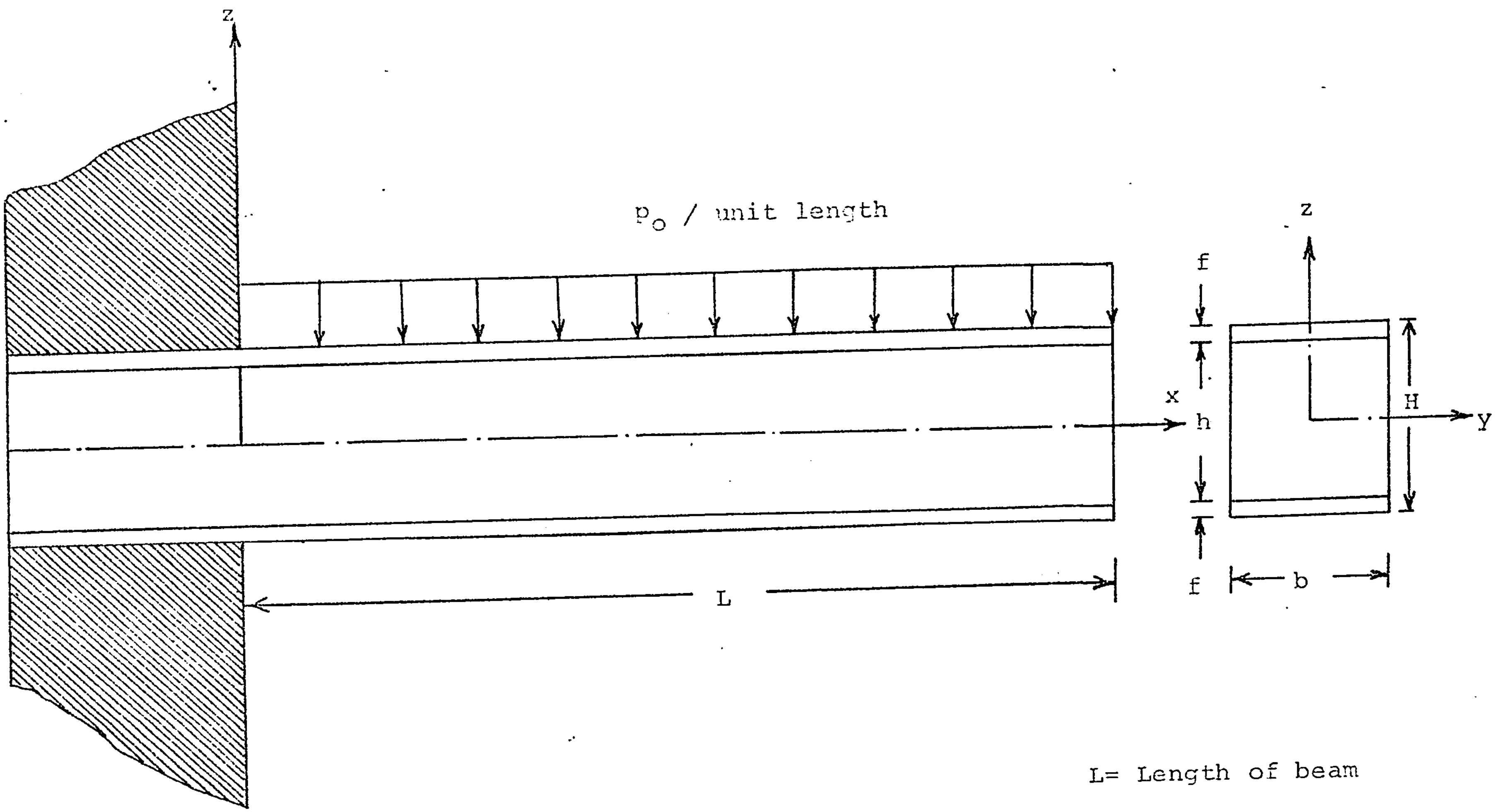


Fig. 1

L= Length of beam

f= Face thickness

h= Core thickness

b= Width of beam

Also, the four constants $a_7$, $a_8$, $a_9$ and $a_{10}$ of the axial deformation function

$$u(x) = a_7 + a_8 x + a_9 x^2 + a_{10} x^3 \qquad (2.2)$$

can be determined in terms of the four nodal quantities $u_1$, $u_{x1}$, $u_2$ and $u_{x2}$. Thus the generalized co-ordinates for the sandwich beam element are:

$$\{w\}^T = (w_1, w_{x1}, w_{xx1}, u_1, u_{x1}, w_2, w_{x2}, w_{xx2}, u_2, u_{x2}) \qquad (2.3)$$

The quantities $u_x$, $w_x$ and $w_{xx}$ mentioned above, denote the derivatives of u and w with respect to x.

II.1 The basis for the formulation of a problem in finite elements is the strain energy expression for a typical element and the potential due to the external loads on this element. The expressions for the strain energy in the core and faces of the sandwich beam element are given in the following sections.

II.1.a Face sheet considerations:

The face sheets of the sandwich material are assumed to be thin isotropic layers of equal thickness (f) and are symmetrically situated with respect to the neutral axis of the beam. In this analysis, only a three-layer sandwich material is considered. It follows from the thin-sheet assumption that the normal stresses in the faces are uniform and the shear strains are zero. It is also assumed that there is no slip between the core and the faces at the interfaces.

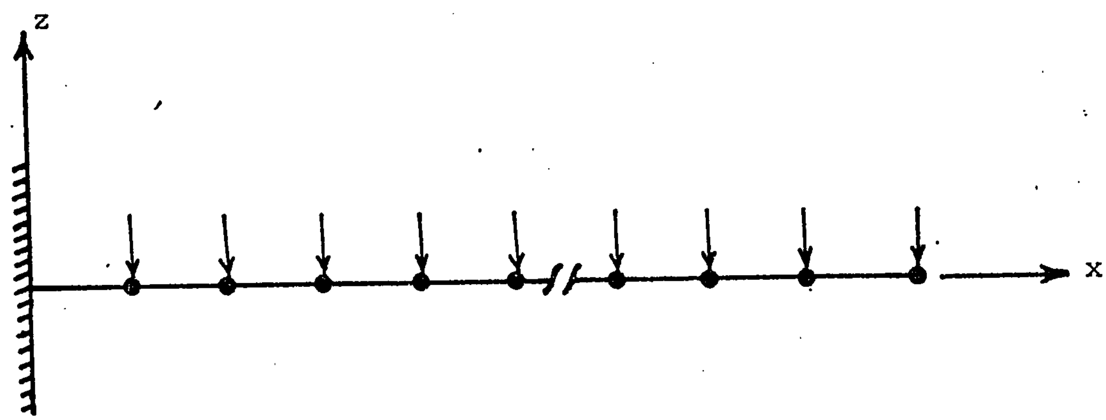


Fig.2 Finite Element Idealization of the Beam.

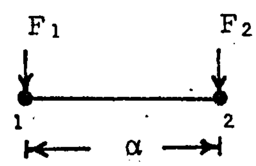


Fig.3 Beam Element Used in this Thesis.

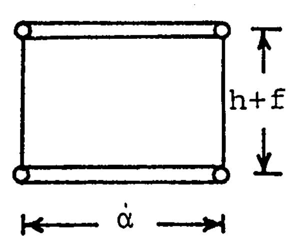


Fig.4 Beam Element used by Maple.

The fundamental relationships for the face sheets can be written as,

$\varepsilon_f = u_x$ the axial strain *

$\sigma_f = E_f \varepsilon_f$ the normal stress

where $E_f$= Young's Modulus of the face material.

The strain energy for each face sheet in a sandwich element of length $\alpha$ is given by,

$$U_f = \frac{1}{2} \int_0^{\alpha} ( A_f u_x^2 + D_f w_{xx}^2 ) \, dx \qquad (2.4)$$

where

$A_f = E_f bf$

$D_f = E_f bf^3/12$

$f$ = thickness of each face sheet

$b$ = width of the sandwich element

Therefore the total strain energy in a sandwich element due to two face sheets is

$$U_{f_{el}} = \int_0^{\alpha} ( A_f u_x^2 + D_f w_{xx}^2 ) \, dx \qquad (2.5)$$

The two terms in the above integrands are contributions of axial and bending strains in the face sheets.

### II.1.b Core considerations

The following assumptions are made in the case of the isotropic core material of the sandwich.

1. The core is incompressible in the transverse direction

---

* Subscript f denotes the quantities associated with the face sheets.

2. The face-parallel shear and extensional stiffnesses are neglegible compared to the transverse stiffnesses.

3. The face-parallel displacements vary linearly across the thickness of the core. In other words, sections which were plane before bending remain plane after bending.

From the assumption that face-parallel stresses are zero in the core, it follows that the shear stresses in the core are independent of the co-ordinate z.

With these assumptions the following relations for the core behavior can be obtained.

$$u_c(x,z_c) = u_{co} + z_c\phi_c^{*} \qquad (2.6)$$

$$\phi_c = (2u + fw_x) \qquad (2.7)$$

$$\gamma_{cxz} = (2u + (h+f)w_x)/(h+f) \quad ^{**}(2.8)$$

$$\tau_{cxz} = G_c\gamma_{cxz} \qquad (2.9)$$

where

$u_{co}$ = mid-core deformation

$\phi_c$ = slope of the elastic curve

$\gamma_{cxz}$ = shear strain in the core (x-z plane)

$\tau_{cxz}$ = shear stress in the core (x-z plane)

Reference is made to Fig. 1 for the co-ordinate system. Due to the assumptions made about the core behavior, it is justifiable to write the total strain energy stored in the core as equal to the distortion energy due to transverse shear. Hence we write,

$$U_{cel} = \frac{G_c bh}{2(h+f)^2}\int_0^{\alpha}(2u + (h+f)w_x)^2 dx \qquad (2.10)$$

* Subscript c denotes quantities associated with the core.
** Approximation used by Reissner[14] for shear strain in the core.

The total strain energy for the sandwich beam element is,

$$U_{el} = U_{f_{el}} + U_{c_{el}}$$

which can be written from equations (2.5) and (2.10) as,

$$U_{el} = A_f \int_0^{\alpha} u_x^2 dx + D_f \int_0^{\alpha} w_{xx}^2 dx + \frac{Gcbh}{2(h+f)} \int_0^{\alpha} (2u+(h+f)w_x)^2 dx \qquad (2.11)$$

## II.2 Potential energy due to external loads:

The potential energy of the applied loads on a beam element of length $\alpha$ can be expressed as,

$$W_{el} = \int_0^{\alpha} H(x)\,u(x)\,dx - \int_0^{\alpha} p(x)\,w(x)\,dx \qquad (2.12)$$

where

$H(x)$ = axial load on the element

$p(x) = p_o$ uniform transverse load on the element

After calculating the potential for an element and then linking the N elements together, the total potential energy of the entire beam can be obtained. This, after minimization, will lead to an approximate solution of the problem. The minimization of total energy is discussed in the section on boundary conditions.

## II.3 Boundary conditions

As mentioned in the introductory chapter, the boundary conditions for this problem are stipulated in terms of displacements. The variational principle may be applied, at this stage, on the total energy of the beam to understand the limitations of classical boundary conditions in details.

The total strain energy of the sandwich beam is obtained by changing the limits of integration in equation (2.11) to L, the overall length of the beam, as

$$U = A_f \int_0^L u_x^2 dx + D_f \int_0^L w_{xx}^2 dx + \frac{G_c bh}{2(h+f)^2} \int_0^L (2u+(h+f)w_x)^2 dx$$

which on expansion becomes,

$$U = A_f \int_0^L u_x^2 dx + D_f \int_0^L w_{xx}^2 dx + \frac{2G_c bh}{(h+f)^2} \int_0^L u^2 dx + \frac{2G_c bh}{(h+f)} \int_0^L u w_x dx + \frac{G_c bh}{2} \int_0^L w_x^2 dx$$

The potential energy of the beam is given by equation (2.12),

$$W = \int_0^L H(x) u(x) dx - \int_0^L p(x) dx$$

The total potential energy of the sandwich beam is then equal to,

$$U_t = U + W$$

$$U_t = A_f I_1 + D_f I_2 + \frac{2G_c bh}{(h+f)^2} I_3 + \frac{2G_c bh}{(h+f)} I_4 + \frac{G_c bh}{2} I_5 + I_6 + I_7 \qquad (2.13)$$

where

$$I_1 = \int_0^L u_x^2 dx, \quad I_2 = \int_0^L w_{xx}^2 dx, \quad I_3 = \int_0^L u^2 dx, \quad I_4 = \int_0^L u w_x dx$$

$$I_5 = \int_0^L w_x^2 dx \quad , \quad I_6 = \int_0^L H(x)\,u(x)\,dx \quad , \quad I_7 = -\,p_o \int_0^L w(x)\,dx$$

The equations of equilibrium can be derived from the requirement that the first variation of the total energy must vanish.

i.e $\delta U_t = \delta(U+W) = 0$

Equation (2.13) is operated with $\delta$ to obtain the first variation of the total potential energy with respect to u and w as,

$$\delta I_1 = \left\{ 2u_x\ \delta u \Big|_0^L - 2 \int_0^L u_{xx} \delta u\ dx \right\}$$

$$\delta I_2 = \left\{ 2w_{xx} \delta w_x \ - [2w_{xxx} \delta w \ - 2 \int_0^L w_{xxxx} \delta w\ dx] \right\}$$

$$\delta I_3 = \ 2 \int_0^L u \delta u\ dx$$

$$\delta I_4 = \left\{ u \delta w \ - \int_0^L u_x \delta w\ dx \ + \int_0^L w_x \delta u\ dx \right\}$$

$$\delta I_5 = \left\{ 2w_x \delta w \Big|_0^L - [2 \int_0^L w_{xx} \delta w\ dx] \right\}$$

Assuming the axial load to be uniform along the length of the beam,

$$\delta I_6 = \int_0^L H \delta u\ dx$$

$$\delta I_7 = - \int_0^L p_o \delta w\ dx$$

Therefore,

$\delta(U+W) = 0$ yields on simplification,

$$\delta(U+W) = \int_0^L \left\{-2A_f u_{xx} + \frac{4G_c bh}{(h+f)^2} u + \frac{2G_c bh}{(h+f)} w_x + H\right\}\delta u \, dx +$$

$$\int_0^L \left\{ 2D_f w_{xxxx} - \frac{2G_c bh}{(h+f)} u_x - G_c bh \, w_{xx} - p_o \right\}\delta w \, dx +$$

$$\Big[2A_f u_x \delta u + 2D_f w_{xx} \delta w_x - 2D_f w_{xxx} \delta w + \frac{2G_c bh}{(h+f)} u\delta w +$$

$$G_c bh \, w_x \delta w\Big]_0^L = 0 \qquad (2.14)$$

In the above equation the quantities within the parantheses must independently vanish. Therefore,

$$A_f u_{xx} - \frac{G_c bh}{(h+f)^2}\{2u + (h+f) w_x\} + \frac{H}{2} = 0$$

$$D_f w_{xxxx} - \frac{G_c bh}{(h+f)} \{2u_x + (h+f) w_{xx}\} - p_o = 0 \qquad (2.15)$$

Equations (2.15) are the equilibrium equations for the sandwich beam. The expression in the square brackets of equation (2.14) gives the boundary conditions for this problem.

The following conditions can be applied to reduce the expression for boundary condition further:

At the fixed end $(x=0)$,

$$u = \delta u = w = \delta w = w_x = \delta w_x = 0$$

At the free end $(x=L)$,

$$w_{xx} = 0 \qquad (2.16)$$

This reduces the natural boundary conditions to,

$$\Big[A_f u_x \delta u - D_f w_{xxx} \delta w + \frac{G_c bh}{(h+f)} u\delta w + \frac{G_c bh}{2} w_x \delta w\Big]_L = 0 \qquad (2.17)$$

Further, if H=0

$u_x = 0$ at $x=L$ and we obtain,

$$\left[D_f w_{xxx} - \frac{G_c bh}{(h+f)} u - \frac{G_c bh}{2} w_x\right]_L = 0 \qquad (2.18)$$

Equations (2.17) and (2.18) are the displacement boundary conditions for the free end of the sandwich cantilever beam. The conditions represented by equation (2.16) are the boundary conditions normally used for the cantilever beams. In the finite element method of analysis in this thesis, only these boundary conditions are used. A further discussion on the possible effects of not satisfying equations (2.17) and (2.18) is given in Chapter V.

II.4 The expression for the strain energy of an element of the sandwich beam, equation (2.11), can in general, be expressed in terms of the displacement vector and stiffness matrices as,

$$U_{el} = \{w\}^T [K_{el}] \{w\} \qquad (2.19)$$

For this problem the matrix $\{w\}$ is a column vector of undetermined nodal parameters as mentioned in equation (2.3), of size 10 x 1. The matrix $[K_{el}]$ is a symmetric matrix of size 10 x 10 , consisting of elements made up of strain energy contributions from the face sheets and core. This matrix is obtained by substituting the displacement functions and their derivatives in the strain energy expression.

We know from Castigliano's theorem that,

$$\frac{\partial U}{\partial w} = F$$

where F ( the force producing deformation w ) is in the direction of the deformation w. This load vector $\{F\}$ can be obtained from the potential energy expression and its components can be considered at the corresponding nodal points. This leads to a consistent load vector of size 10 x 1 for the sandwich beam element. Hence we obtain from equation (2.19),

$$\{F\} = \frac{\partial U_{el}}{\partial \{w\}^T} = \left[K_{el}\right] \{w\} \tag{2.20}$$

for an element.

When the stiffnesses of the individual elements are added together the overall stiffness of the sandwich beam is obtained. Similarly, the consistent load vector elements for the whole beam is assembled. Thus in equation (2.20) the vector {F} and stiffness matrix $\left[K_{el}\right]$ are known quantities. With the appropriate boundary conditions, this equation is solved for the generalized displacements {w}.

The problem formulated above in terms of the strain energy and load potential is solved by going through the following steps in proper sequence.

1. Substitution of assumed displacement functions in the strain energy expression to obtain the element stiffness matrix of the sandwich element.

2. Generation of the consistent load vector elements from the potential energy expression.

3. Assembling the individual element stiffness matrix of each element of the beam to form the overall stiffness matrix of the beam.

4. Assembling of consistent load vector of each element to obtain the overall load representation of the entire beam.

5. Application of suitable displacement boundary conditions and solution of the matrix equation to obtain the nodal displacements.

# III. COMPUTATIONS

III.1 It was found convenient to use the high speed digital computer to generate and solve the matrix equations mentioned in the previous chapter. This eliminated a tedious set of calculations, arising in the integration of the expression for strain energy and potential energy and the subsequent solution of the problem. A computer program in Fortran IV has been developed to solve the problem for various load conditions and parameters. All the computations were carried out in double precision and the elastic continuum was represented by a convenient number of finite elements, dictated by the storage capacity of the computer.

## III.2 Element stiffness matrix

For convenience in computation, the basic relations in the previous chapter were represented in the following series form:

$$w = \Sigma\, a_i x^{m_i} \quad , \quad i = 1 \text{ to } 6$$

and

$$u = \Sigma\, a_i x^{n_i} \quad , \quad i = 7 \text{ to } 10 \qquad (3.1)$$

where the exponents of x, given as $m_i$ and $n_i$ take on the following values:

$m_1=0,\ m_2=1,\ m_3=2,\ m_4=3,\ m_5=4,\ m_6=5$

$n_7=0,\ n_8=1,\ n_9=2,\ n_{10}=3$

Differentiating equations (3.1), the following equations can be obtained:

$$w_x = \Sigma a_i m_i \; x^{(m_i-1)} \qquad , \; i= 2 \text{ to } 6$$

$$w_{xx} = \Sigma a_i m_i (m_i-1) \; x^{(m_i-2)} \qquad , \; i= 3 \text{ to } 6$$

$$u_x = \Sigma a_i n_i \; x^{(n_i-1)} \qquad , \; i= 8 \text{ to } 10 \qquad (3.2)$$

By series multiplication of equations (3.2), the following relations can be easily established.

$$w_x^2 = \Sigma\Sigma a_i a_j m_i m_j \; x^{(m_i+m_j-2)} \qquad , \; i,j= 2 \text{ to } 6$$

$$w_{xx}^2 = \Sigma\Sigma a_i a_j m_i m_j (m_i-1)(m_j-1) \; x^{(m_i+m_j-4)} \qquad , \; i,j= 3 \text{ to } 6$$

$$u_x^2 = \Sigma\Sigma a_i a_j n_i n_j x^{(n_i+n_j-2)} \qquad , \; i,j= 8 \text{ to } 10$$

also,

$$u^2 = \Sigma\Sigma a_i a_j x^{(n_i+n_j)} \qquad , \; i= 7 \text{ to } 10$$

$$\begin{aligned} uw_x = \tfrac{1}{2} \Sigma\Sigma a_i a_j m_j x^{(n_i+m_j-1)} &+ \qquad , \; i= 7 \text{ to } 10; \; j= 2 \text{ to } 6 \\ \tfrac{1}{2} \Sigma\Sigma a_i a_j m_i x^{(m_i+n_j-1)} & \qquad , \; i= 2 \text{ to } 6 \; ; \; j= 7 \text{ to } 10 \end{aligned}$$

$$(3.3)$$

Equations (3.3) can be substituted in the expression for total strain energy given by equation (2.11). Thus, for the total strain energy of the sandwich beam element, we obtain:

$$U_{el} = A_f \int_0^{\alpha} \Sigma\Sigma a_i a_j n_i n_j x^{(n_i+n_j-2)}\, dx \; +$$

$$D_f \int_0^{\alpha} \Sigma\Sigma a_i a_j m_i (m_i-1) m_j (m_j-1)\; x^{(m_i+m_j-4)}\, dx \; +$$

$$G1 \int_0^{\alpha} \Sigma\Sigma a_i a_j x^{(n_i+n_j)} dx \; +$$

$$G2 \int_0^{\alpha} \Sigma\Sigma a_i a_j m_i m_j x^{(m_i+m_j-2)} dx \; +$$

$$G3 \int_0^{\alpha} \Sigma\Sigma a_i a_j m_j x^{(n_i+m_j-1)}\, dx \; +$$

$$G3 \int_0^{\alpha} \Sigma\Sigma a_i a_j m_i x^{(m_i+n_j-1)}\, dx \qquad (3.4)$$

where the following notations have been introduced for the sake of brevity:

$$G1 = 2G_c bh/(h+f)^2$$

$$G2 = G_c bh/2$$

$$G3 = G_c bh/(h+f)$$

The integration in equation (3.4) is carried over the entire length $\alpha$ of one element. It can be seen that, equation (3.4) above exhibits symmetry. This particular property, which structurally is indicative of the theorem of reciprocity, leads to a symmetric stiffness matrix for the beam element and overall symmetry for the stiffness matrix of the assembled structure.

For the convenience in writing and easier computer algorithm, the following definitions are introduced:

$$I_1 = A_f \sum\sum a_i a_j n_i n_j \int_0^{\alpha} x^{(n_i+n_j-2)}\, dx$$

$$I_2 = D_f \sum\sum a_i a_j m_i (m_i-1) m_j (m_j-1) \int x^{(m_i+m_j-4)}\, dx$$

$$I_3 = G1 \sum\sum a_i a_j \int_0^{\alpha} x^{(n_i+n_j)}\, dx$$

$$I_4 = G2 \sum\sum a_i a_j m_i m_j \int_0^{\alpha} x^{(m_i+m_j-2)}\, dx$$

$$I_5 = G3 \sum\sum a_i a_j m_j \int_0^{\alpha} x^{(n_i+m_j-1)}\, dx$$

$$I_6 = G3 \sum\sum a_i a_j m_i \int_0^{\alpha} x^{(m_i+n_j-1)}\, dx$$

With this, the total strain energy given by equation (3.4) reduces to the form given by equation (3.5).

$$U_{el} = I_1+I_2+I_3+I_4+I_5+I_6 \qquad (3.5)$$

In matrix notation, each of these integrands can be expressed as:

$$I_1 = (a_8, a_9, a_{10}) \, [SK]_1 \, (a_8, a_9, a_{10})^T$$

$$I_2 = (a_3, a_4, a_5, a_6) \, [SK]_2 \, (a_3, a_4, a_5, a_6)^T$$

$$I_3 = (a_7, a_8, a_9, a_{10}) \, [SK]_3 \, (a_7, a_8, a_9, a_{10})^T$$

$$I_4 = (a_2, a_3, a_4, a_5, a_6) \, [SK]_4 \, (a_2, a_3, a_4, a_5, a_6)^T$$

$$I_5 = (a_7, a_8, a_9, a_{10}) \, [SK]_5 \, (a_2, a_3, a_4, a_5, a_6)^T$$

and

$$I_6 = (a_2, a_3, a_4, a_5, a_6) \, [SK]_6 \, (a_7, a_8, a_9, a_{10})^T \qquad (3.6)$$

In the above equations, the matrices $[SK]_i$ are generated by performing the following integrations:

$$SK_1 = A_f\, n_i n_j \int_0^d x^{(n_i+n_j-2)}\,dx \qquad , \; i = 8 \text{ to } 10,\; j = 8 \text{ to } 10$$

$$SK_2 = D_f\, m_i(m_i-1)\,m_j(m_j-1) \int_0^d x^{(m_i+m_j-4)}\,dx \qquad , \; i=3 \text{ to } 6,\; j=3 \text{ to } 6$$

$$SK_3 = G1 \int_0^d x^{(n_i+n_j)}\,dx \qquad , \; i = 7 \text{ to } 10,\; j = 7 \text{ to } 10$$

$$SK_4 = G2\, m_i m_j \int_0^d x^{(m_i+m_j-2)}\,dx \qquad , \; i = 2 \text{ to } 6,\; j = 2 \text{ to } 6$$

$$SK_5 = G3\, m_j \int_0^a x^{(n_i+m_j-1)}\,dx \qquad , \; i = 7 \text{ to } 10,\; j = 2 \text{ to } 6$$

$$SK_6 = G3\, m_i \int_0^d x^{(m_i+n_j-1)}\,dx \qquad , \; i = 2 \text{ to } 6,\; j = 7 \text{ to } 10$$

It can be shown that the total strain energy expression is equivalent to the following matrix equation.

$$U_{el} = \{A\}^T [SK] \{A\} \qquad (3.7)$$

where

$$\{A\}^T = (a_1, a_2, a_3, \ldots\ldots\ldots, a_{10})_{10 \times 1}$$

and

$$[SK] = \left[\begin{array}{c|c} [SK_2]+[SK_4] & [SK_6] \\ \hline [SK_5] & [SK_1]+[SK_3] \end{array}\right]_{10 \times 10}$$

It can be easily verified that, in the matrix $[SK]$, the partitioned components $[SK]_i$ have the following meaning:

$[SK]_2$ and $[SK]_4$ contribute towards the transverse deformation w and its derivatives $w_x$ and $w_{xx}$.

$[SK]_1$ and $[SK]_3$ influence the axial deformation u and its derivative $u_x$.

$[SK]_6 = [SK]_5^T$ represents the cross influence of u and w. The vector {A} can be expressed in terms of the generalized displacement vector {w} as:

$$\{A\} = [T]^{-1}\{w\} \qquad (3.8)$$

where [T] is the transformation matrix involving the linear dimensions of the beam element. The matrix [T] can be shown to be,

$$[T] = \begin{bmatrix} 1 & 0 & 0 & 0 & 0 & 0 & 0 & 0 & 0 & 0 \\ 0 & 1 & 0 & 0 & 0 & 0 & 0 & 0 & 0 & 0 \\ 0 & 0 & 2 & 0 & 0 & 0 & 0 & 0 & 0 & 0 \\ 0 & 0 & 0 & 0 & 0 & 0 & 1 & 0 & 0 & 0 \\ 0 & 0 & 0 & 0 & 0 & 0 & 0 & 1 & 0 & 0 \\ 1 & \alpha & \alpha^2 & \alpha^3 & \alpha^4 & \alpha^5 & 0 & 0 & 0 & 0 \\ 0 & 1 & 2\alpha & 3\alpha^2 & 4\alpha^3 & 5\alpha^4 & 0 & 0 & 0 & 0 \\ 0 & 0 & 2 & 6\alpha & 12\alpha^2 & 20\alpha^3 & 0 & 0 & 0 & 0 \\ 0 & 0 & 0 & 0 & 0 & 0 & 1 & \alpha & \alpha^2 & \alpha^3 \\ 0 & 0 & 0 & 0 & 0 & 0 & 0 & 1 & 2\alpha & 3\alpha^2 \end{bmatrix} \quad 10 \times 10$$

so that,

$$\{w\} = [T]\{A\}$$

Substitution of equation (3.8) into (3.7) yields

$$U_{el} = \{w\}^T [T^{-1}]^T [SK] [T^{-1}] \{w\}$$

The total energy is now expressed in terms of the displacement and stiffness matrices as,

$$U_{el} = \{w\}^T [SM] \{w\} \qquad (3.9)$$

where

$$[SM] = [T^{-1}]^T [SK] [T^{-1}]$$

The matrix [SM] is the stiffness matrix of the beam element. It is clear that [SM] will be a symmetric matrix, since [SK] is a symmetric matrix.

Thus, if the integrations involved in the computation of [SK] are carried out, the stiffness matrix [SM] can be obtained by pre-multiplying and post-multiplying [SK] by the inverse transpose and inverse of matrix T respectively. A program was developed to generate the elements of the stiffness matrix, the listing of which is given in the Appendix.

## III.3 Consistent load vector

At this stage, Castigliano's theorem can be applied, which will yield the load vector corresponding to the generalized displacement vector {w} . This is achieved by differentiating equation (3.9) with respect to the generalized displacement vector and realising that the displacements are in the direction of the applied forces. From equation (3.4) we write,

$$\frac{\partial U_{el}}{\partial \{w\}^T} = \{F\} = [SM] \{w\} \qquad (3.10)$$

In the above equation, the load vector {F} can be evaluated from the knowledge of the loading conditions and from the potential energy expression ( 2.12 ). In the above expression the load vector {F} , like the displacement vector {w} is used in the general sense and therefore the elements of {F} include moments, torques etc. These elements can be written as,

$$\{F\} = ( F_{t_1}, M_1, C_1, F_{a_1}, F_{ax_1}, F_{t_2}, M_2, C_2, F_{a_2}, F_{ax_2})$$

where

$F_{ti}$ = external shear forces causing deformations $w_i$ at nodes i=1 and 2, with proper units.

$M_i$ = external couples producing slopes $w_{xi}$ at the two nodes of the beam element.

$C_i$ = fictitious torques causing curvatures $w_{xxi}$ at nodes 1 and 2, with proper dimensions.

$F_{ai}$ = the axial loads responsible for the axial deformation $u_i$ at the nodes.

$F_{axi}$ = fictitious axial force quantity causing $u_{xi}$ at the nodes.

The subscripts t and a, are used to represent the transverse and axial components of the load at the nodes.

Equation (2.12) representing the potential energy in an element due to the external loads, can again be written in matrix form in the following manner. In the absence of the axial forces, equation (2.12) can be written as,

$$W_{el} = -p_o \int_0^{\alpha} w(x)\,dx \qquad (3.11)$$

where $p_o$ is the intensity of the uniformly distributed transverse load. Equation (3.11) can be written in the form of a series by substituting the expression for w from equation (3.1).

$$W_{el} = -p_o \int_0^{\alpha} a_i x^{m_i}\,dx \;, \; i = 1 \text{ to } 6 \qquad (3.12)$$

Substituting for $a_i$ from equation (3.8) and rewriting (3.11) in matrix form, it can be shown that

$$W_{el} = \{w\}^T [T]^{-1} \{P\} \qquad (3.13)$$

where the vector {P} is defined as,

$$\{P\} = p_o \, \alpha^{m_i+1} / (m_i+1) \qquad (3.14)$$

Equation (3.14) can, now be written in a form utilizing the concept of consistent load vector {F} as,

$$W_{el} = \{w\}^T \{F\} \qquad (3.15)$$

where

$$\{F\} = [T]^{-1} \{P\} \qquad (3.16)$$

Differentiating equation (3.15) with respect to the generalized displacement vector {w} we get,

$$\frac{\partial W_{el}}{\partial \{w\}^T} = \{F\}$$

by Castigliano's theorem.

It is clear from equations (3.14) and (3.16) that the elements of the consistent load vector {F} can be easily generated with the knowledge of the load intensity, and the size of the beam element.

III.4 Assembling the overall structural stiffness matrix

Once the stiffness of a single element of the beam is known, the overall stiffness of the entire beam can be computed by assembling these individual stiffnesses. A subroutine was written for this computation and the listing is included in the Appendix. A similar approach is followed in computing the overall consitent load vector for the beam.

III.5 Boundary conditions

The boundary conditions in this problems are displacement boundary conditions, rather than stress boundary conditions. These boundary conditions are discussed in Chapter II and an algorithm has been developed to apply these conditions at the nodes corresponding to the fixed end and the free end of the beam. If, for example, $w_x$ at node 1 is to be set to zero, this is achieved by substituting zeros in the corresponding rows and columns, and writing unity in the diagonal element of the overall structural stiffness matrix $[SS]$. The corresponding element in the overall consistent load vector $\{VL\}$ is also set to zero.

## III.6 Solution of the problem

The problem now is to solve the following matrix equation:

$$\{VL\} = [SS]\{w\} \tag{3.17}$$

In this work, the beam was divided into 32 elements, giving rise to an overall stiffness matrix of size 165 x 165. A standard matrix inversion routine was used to solve this system of linear equations. The formal solution of the generalised displacement vector $\{w\}$, from equation (3.17), is given as

$$\{w\} = [SS]^{-1}\{VL\}$$

# IV. EXPERIMENTATION

IV.1 The experimentation in this project consists of the measurement of the transverse deformation of the sandwich beam and of the stresses at a typical cross-section. The photoelastic tachnique was used to determine the stress distribution very close to the fixed end of the cantilever beam. A highly sophisticated photoelastic polariscope was used for this purpose. This polariscope has a precision table for mounting two-dimensional models and the table movements can be controlled by means of micrometer verniers having an accuracy of 0.0001". This feature of the machine was made use of in the measurement of transverse deformations in the models. A brief description of the polariscope assembly is given below.

a. Optical system

This provides a collimated vertical light path and has the following parts.

1. A point light source cooled by a fan
2. Collimating lens system
3. Observation screen with hood
4. Objective lens with magnifications of 10 and 20
5. Control for light intensity
6. Additional light source for reflection accessory

b. Precision table

This is a two-stage x-y measuring table with an overall travel of 4" x 1", and carries a micrometer adjustment with an accuracy of 0.0001" in both directions. This table supports the two-dimensional models perpendicular to the path of light.

c. Polariser assembly

This carries the polariser, analyser and the two quarter-wave plates mechanically coupled together. For isoclinic work all these four parts can be rotated together. During isoclinic observations, the quarter-wave plates can be moved out of the field by a simple rotation of a handle. For isochromatic work a rotation in the opposite direction would bring the quarter-wave plates into the field. This ease of operation enables quick observation of the relevent data at any given point. Further, the independent rotation of the analyser to an accuracy of 1 degree provides for Tardy compensation.

d. Straining frame

This rigid feature is extremely useful in cases of tensile and compressive loading of photoelastic specimens. This is a constant deflection system designed to load the photoelastic models up to 500 lbs. However, for this investigation another loading arrangement had to be designed which is dicussed on page 37.

e. Accessories

The photoelastic polariscope has the following accessories.

i. Photographic accessory: The ground glass screen on which the photoelastic fringe and isoclinic patterns are observed, can be replaced by a 4" x 5" photographic attachment. This enables a permanent record of experimental data for future reference.

ii. Monochromator: This feature aids in identifying the fringe pattern by cutting out the dispersed band of colours and providing sharp dark fringes.

iii. Uniform field compensator: This is helpful for the cases where it is difficult to identify the fringe orders by sheer visual observation of the pattern as it is formed. A calibrated scale provides for the identification of fractional and integral fringe orders, in this instrument.

iv. Oblique incidence attachment: This is a combination of prisms, through which polarised light is deflected to pass through the model. With the help of this arrangement, both direct and oblique incidence readings can be obtained. A combination of these readings is sufficient to determine the principal stresses.

## IV.2 Photoelastic model materials and cements

a. Model materials: The materials used in the models of the sandwich beam go by the commercial names PSM-1 and PSM-4.

These were purchased in the form of sheets of size 10" x 10" and nominal thickness of 0.25".

i. PSM-1 : This is a clear polyester sheet, free from creep and edge effects and has the following properties.

Modulus of elasticity $E = 323{,}000$ psi. *

Poissons ratio $\nu = 0.38$

Stress optic constant = 36 psi/fringe/inch*

This material was used as face sheets in the sandwich beams.

ii. PSM-4 : This is a polyurethane sheet having a very low elastic modulus. It has the following properties.

Modulus of elasticity $E = 1000$ psi.

Stress optic constant = 1.186 psi/fringe/inch *

b. Cements: The cement chosen for bonding the face sheets to the core material has an elastic modulus of $E = 30{,}000$ psi. The cement is prepared by combining a resin and a hardener which have the commercial names PC-6C and PCH-6 respectively.

## IV.3 Procedure for preparation and handling of specimens

The photoelastic technique necessitates much care in the fabrication and handling of models. The machining operations were carried out using sharp tools and special fixtures at high speeds. The dimensions and squareness of the models were maintained with greatest possible care. Problems were encountered in this respect in the machining of PSM-4, because of its high flexibility and softness**. Low depths of cut were given at steady

---

* Values obtained experimentally. The unstarred values are from the supplier's literature.

** More details on the machining of model materials are given in Section IV.11, p.50a .

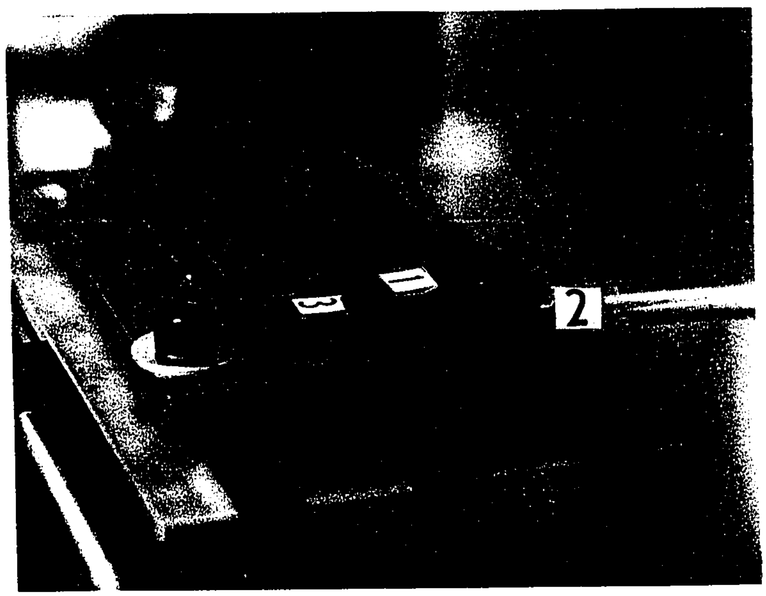


Fig.5 Loading Rig No.1

1. Enclosure for balloon
2. Connecting tube from air reservoir
3. Beam model in position

and continuous feeds during the milling operations to eliminate machining stresses.

The face sheets (PSM-1) were bonded to the core material with extreme care and the procedure recommended in the literature was closely adhered to. The models were allowed to cure for 24 hours at room temperature as recommended in the literature. It was found necessary to keep the models at a mild uniform pressure for a few hours so as to let the face sheets stick firmly to the cores of the beams.

## IV.4 Loading technique

The straining frame described earlier is not adequate to handle situations wherein a bending load is to be applied. A special fixture was developed to achieve uniformly distributed loading. Two factors were to be reckoned with in designing such a fixture. First of all, the very nature of the polariscope dictated a fixture capable of allowing bending in the horizontal plane. In the second place, very limited space was available to accommodate the fixture. These factors were carefully considered in the design of the loading rig. It was felt that the same design features could be more effectively achieved on a bench type polariscope.

In the initial phases of the project, application of air pressure was thought to be an appropriate method to achieve uniformly distributed loading. An all-brass fixture was designed and fabricated to obtain this type of loading. This fixture, shown in Fig.5, was designed to hold the rigidly clamped sandwich beam in position. The beam lying flat with its lateral and longitudinal axes in the horizontal plane, was allowed to slightly enter the recess ( 1 in Fig.5 ) of the fixture. Air pressure was applied to this edge of the beam through an inflated, but constricted rubber balloon. A mercury manometer with sufficient controls was designed to measure the air pressure and an air-filled gas cylinder was used as air reservoir. The principle involved is much the same as that in the case of an automobile tire-tube combination which supports the weight of the whole vehicle. Such an enclosed tube would transmit the pressure of the medium inside, without supporting the same by its skin. In this case, the skin of the constricted balloon ( restricted by the brass enclosure on three sides and by the edge of the sandwich beam on the fourth ) transmits the air pressure on to the beam and thereby bends it. Such a method of simulating uniformly distributed loading was successfully employed by Durelli, Lake and Tsao [4] in applying uniform load on a plate under compression. However, it was found that this method would not work out satisfactorily in the case of beam bending problems. Further, in the case of sandwich cantilever beams, the deflections were large enough to allow the balloons to escape through the open space created between the deformed configuration of the beam and the frame, resulting in the breaking of the balloons. Several attempts were made to improve upon this fixture, but due to the large deflections in the beam, it

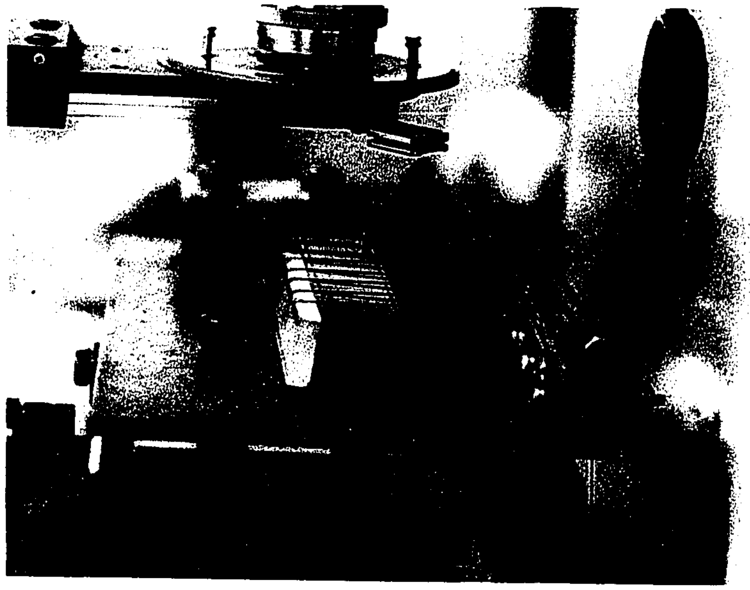

Fig.6 Loading Rig No.2 ( Analyser in view )

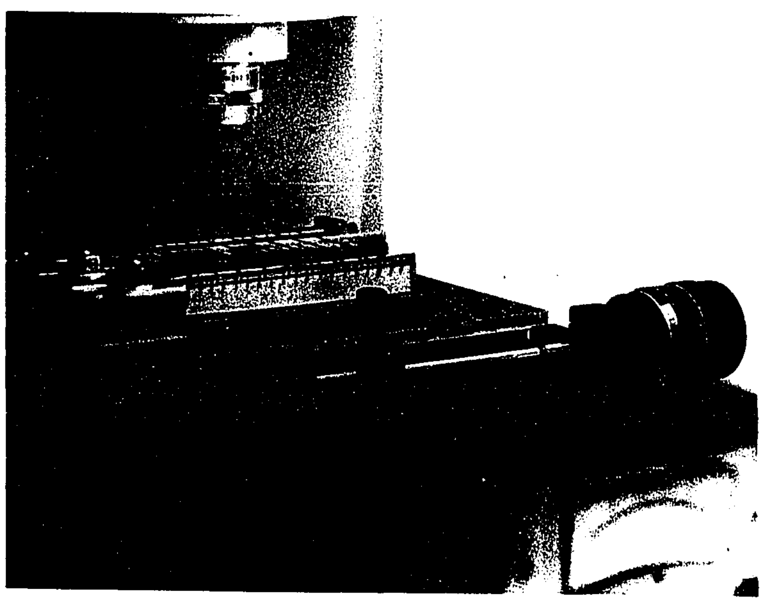

Fig.7 Loading Rig No.2 ( another view )

was felt that, some basic changes must be incorporated. Therefore, no experiments were performed with Loading Rig No. 1.

Another fixture was designed and fabricated to obtain uniformly distributed loading. This, shown in figures 6 and 7. is a mechanical means of applying uniformly distributed load to a beam. This consists of a ¼" steel plate ( Refer to Fig.8 ) with a cut-out portion to let the polarised light pass through. It carries two steel angles supporting a ¼" diameter brass cylinder. The steel plate can be mounted and bolted on to the polariscope table. The beam can be rigidly fixed with the help of the support plates on to the table of the polariscope. When the beam is mounted on the fixture, its bottom surface is in plane with a series of equally spaced holes on a rigid plate, which is fixed to the steel angles. The top surface of the beam is aligned with the top surface of the brass cylinder. This enables a set of equally spaced strings, carrying loads, to be passed around the beam. The strings are held in position on to the rigid plate carrying the equi-spaced holes. Thus, a number of loads can be applied at discrete points along the length of the beam. In this manner, an approximation to a uniformly distributed loading can be achieved.

In this case, further improvements towards a better dispersion of the load were made by placing a very soft polyurethane strip (PSM-4) on the loaded face of the beam. The number of strings, and hence loads were limited by the space available in the recess of the polariscope. It was possible

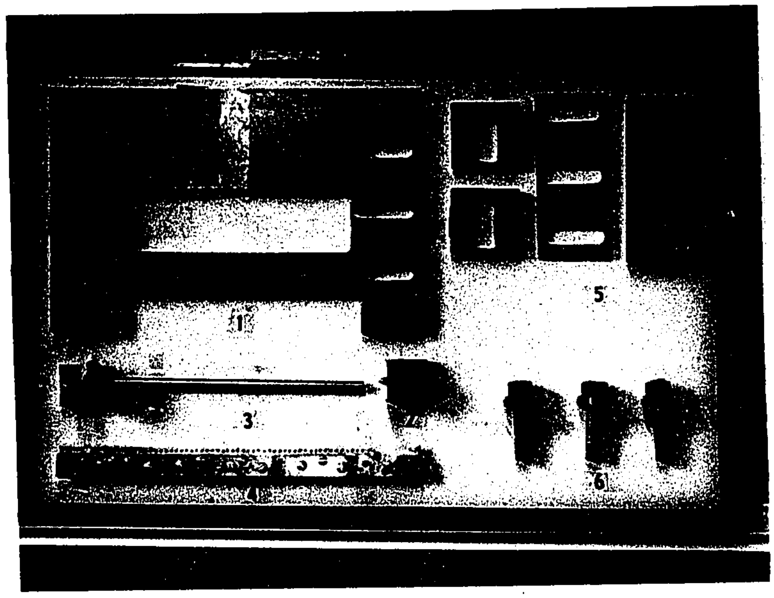

Fig.8 Components of Loading Rig No.2

1. Steel plate
2. Steel angle
3. Brass cylinder
4. Plate with equally spaced holes
5. Support plates
6. Securing bolts

to use ten load-carrying strings along the length of the beam. Two strings were used to carry one unit of loading "weights" through a V-shaped arrangement. This resulted in the application of 2 lbs. of load over a length of 5.25 inches or an intensity of 0.3809 lb/in. Such awkward value for the loading could not be helped, as choice of load intensity was influenced by other factors, discussed in a later section of this chapter.

IV.5 Handling of loads

Unlike the straining frame, there were no provisions to apply the load gradually or to apply additional loads in the above set up. A device had to be made to apply the load gradually, so that the fringe formation could be traced and at the same time avoid the dynamic effects of the loads. An extended screw jack was used to raise and lower the loads gradually during the experimentation. This made the checking and rechecking of the fringe orders possible, which was absolutely necessary because of the duality of material in the sandwich beam.

IV.6 Choice of loads

The limit on the intensity of loading was set by two factors - in the first place, by the properties and dimensions of the beam and in the second place by the space available on the polariscope. The materials used in the sandwich beam have stress optic constants of 36 psi/fringe/inch and about 1.2 psi/fringe/inch. This means that, if a medium order of fringe is formed in the thin face sheets, the order of fringes in the soft thick core will go beyond the range of the uniform field compensator. On the other hand, low fringe orders in the core would be at the cost of very low orders in the face sheets. A compromise had to be struck to obtain sufficiently high order fringes in both core and face sheets.

The working space available to accommodate and handle loads was very limited. The loads were to be small in size to hang freely without touching one another. Further, they should not touch or rest against the body of the polariscope at any position of the machine table. Weights with hooks, as used with chemical balances, were an easier choice from the point of view of handling, but these were found to occupy a larger space and therefore, thin metallic discs with slots, having calibrated weights were selected.

## IV.7 Model dimensions

The dimensions of the models depended on the field of the polariscope and machining considerations. The field of the polariscope restricted the beam length to less than 5½" and width to not more than 1¼". Machining considerations limited the core width to a minimum of 0.625" and face thickness to a minimum of 0.0625". With these considerations, five models of sandwich beams were made, whose dimensions are given in Table I.

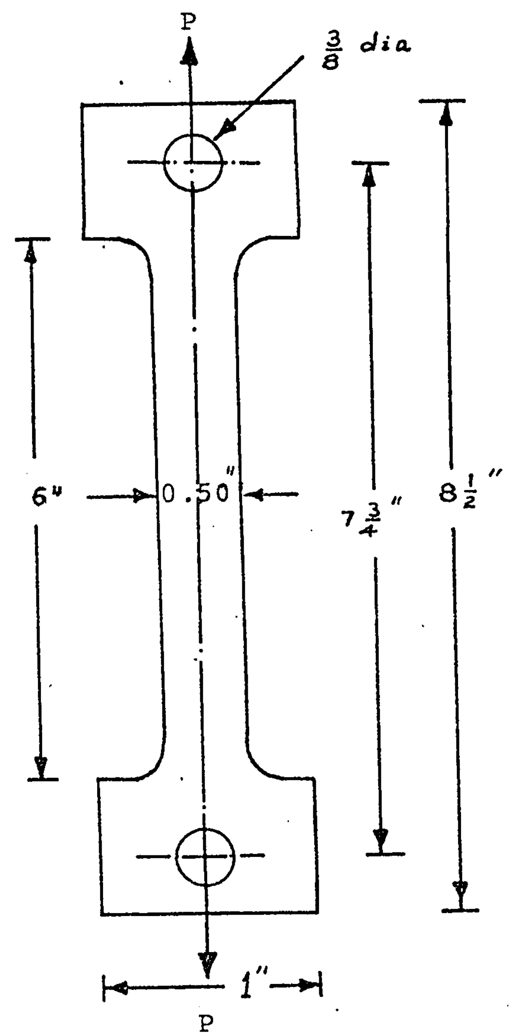


Fig.9 Calibration Specimen

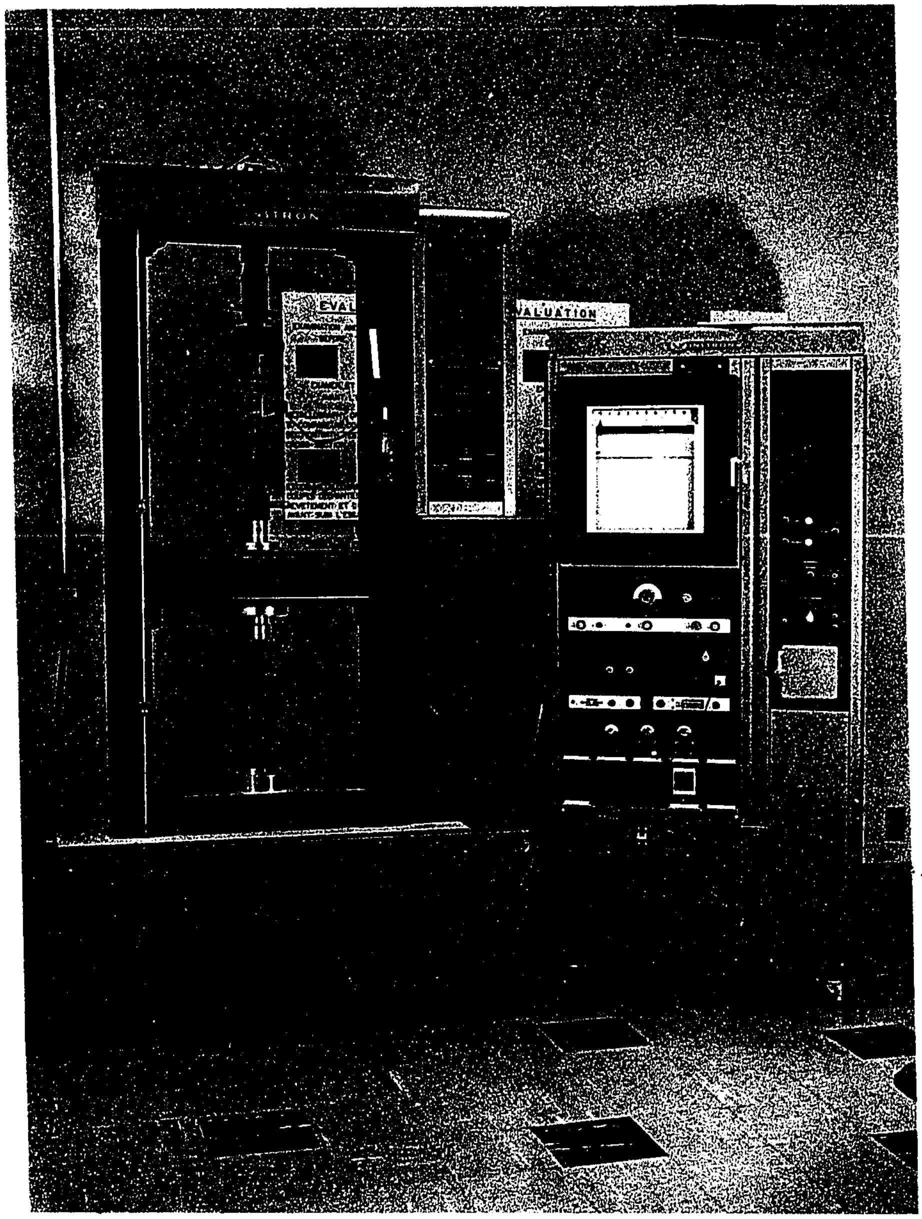

Fig.10 Tensile Test Set Up

## IV.8 Calibration of models

The stress optic coefficients for the materials PSM-1 and PSM-4 were determined experimentally, as variations in their properties with time, temperature are known to exist. A tensile test specimen as shown in Fig.9 was used. For the hard plastic the straining frame and load cell readout unit were used and load vs. fringe order was plotted and from this the stress optic coefficient was determined. In the case of the soft plastic, very small loads were enough to produce sufficient orders of fringes. These loads could not be established and read accurately with the straining frame unit. Therefore, a simple pulley arrangement was made to apply small loads gradually. A plot of load vs. fringe order was made in this case also, and the stress optic coefficient of the material was determined.

## IV.9 Tensile test on the model material

It was found necessary to accurately determine the modulus of elasticity of the model materials, by carrying out tensile tests on specimens. For this purpose, the Instron Testing Machine at the Materials Laboratory of the National Research Council of Canada, Ottawa was used. A sketch of the test specimen and photographs of the experimental set up are given on pages 44, 45 and 47. In the case of the soft plastic this machine could not be used because of the non availability of a very low-range load cell. Hence, the catalogue value of

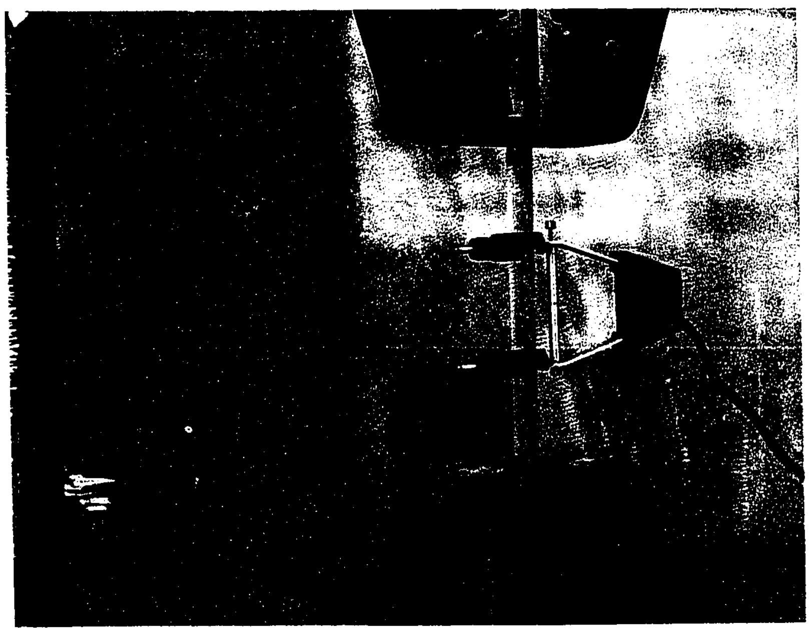

Fig.11 Tensile Test Model with Extensometer

E = 1000 psi has been used in the numerical computations.

IV.10. Experimentation - Procedure and analysis of data

The sandwich beam model was mounted on the loading rig, and the axis was aligned with the horizontal cross wire in the observation screen of the polariscope. After rigidly clamping the beam in this position , load was applied to the beam using the special jack.

A typical section was selected close to the fixed end of the beam. The isoclinic and isochromatic data were taken along lines OP, AB and CD ( Fig.12 ). These data were taken at equal steps of 0.025" starting from the free boundary. The uniform field compensator was used to identify the fringe orders at each point. The special provision in the machine to put the quarter-wave plates out of the field, was made use of to read the isoclinic parameter at every point, just before reading the fringe order.

To obtain the stress distribution from these data, the shear difference method was used. This method of separation of stresses is outlined in the Appendix. A listing of the computer program for applying this method is also included in the Appendix.

The transverse deformations were measured along the length of the beam. To start with, the reading corresponding to the undeformed positition of the neutral axis was read using the vernier micrometer. After application of the load, readings of the deformed configuration of the beam were taken at previously

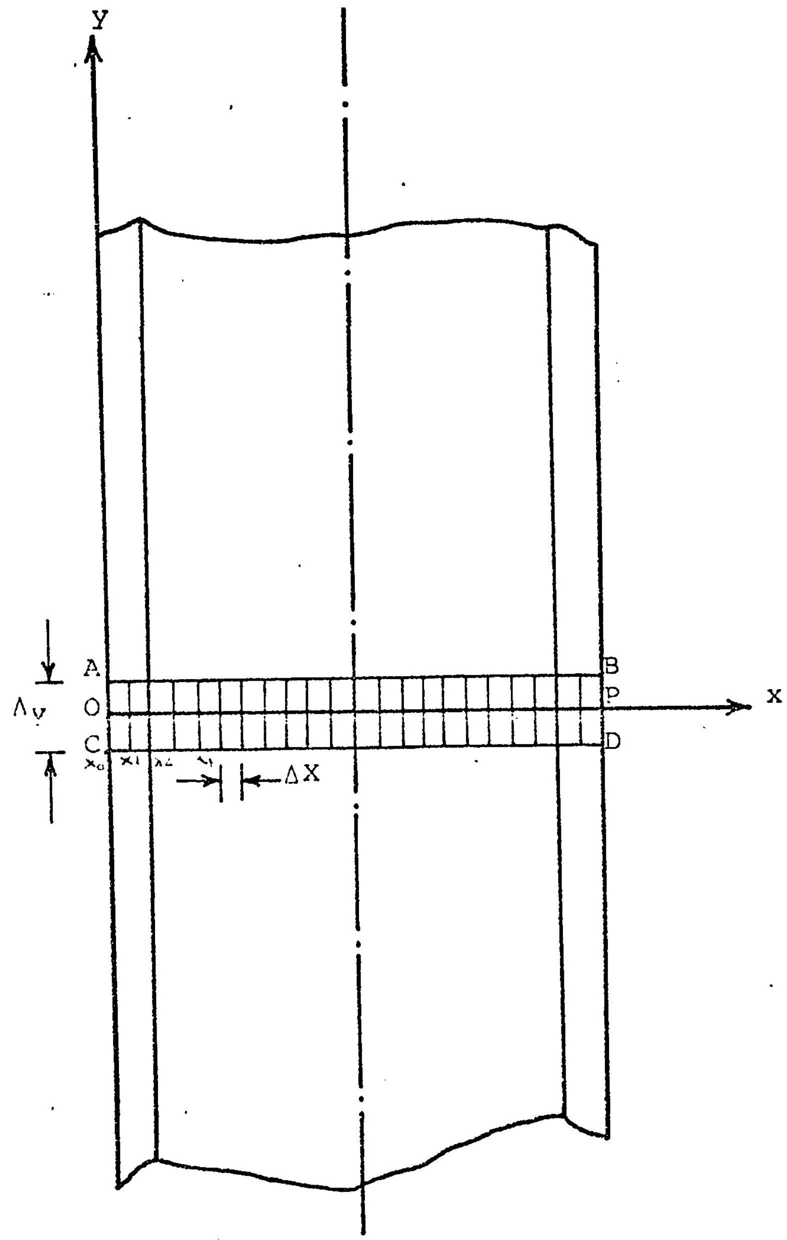


Fig. 12 Grid System for Shear Difference Method

marked stations along the length of the beam. The difference between these two readings is the deformation of the beam.

Color photographs of the fringe pattern were taken at typical sections of the beam. A set of four pictures of these is shown on pages 80 and 81. The isochromatics are shown in figures 33, 34 and 36. These are parallel lines in the face sheets and wide bands of color in the core. Fig.35 shows the 45 degree isoclinic in the core along with the isochromatics in the face sheet. In all these pictures the white patch of light observed is from an extraneous source during the printing process.

## IV.11 Machining of model materials

The machining of the thin face sheets and the soft core for the sandwich beams required special methods of clamping. The face sheets were to be thin (1/16") and of uniform thickness. The PSM-1 sheets used in this case were first cut in a scroll saw with sufficient machining allowance. The final machining was carried out in a milling machine. A set of six strips of these sheets were clamped together and the finishing cut was given at a slow and steady feed, with a depth of cut not exceeding 0.005".

In the case of the soft.plastic (PSM-4), a slightly different method of clamping was required because of its high flexibility. Strips were first cut in the scroll saw with large machining allowances and the final machining was done in a milling machine. The strips were kept in between sheets of hardboard on which the final dimensions were marked. This set up was clamped on the milling machine vise, and the milling was carried out at a slow and steady feed. During this milling process the hardboards on both sides were also machined.

The literature recommends freezing of PSM-4 before machining operations. However, it was not possible to maintain the material frozen throughout the milling operation. The heat generated during the machining process made this impossible and hence the method described in the previous paragraph was adopted.

## V. DISCUSSION OF RESULTS AND CONCLUSIONS

Experiments were performed on five sandwich beams to determine the stress distribution across their depth, using the photoelastic technique. The results obtained are plotted in figures 18 to 22. The relative dimensions of these beams are given in Table I. The section chosen to find the stress distribution was near the fixed end of the beam. This was done to exclude the effects of local compression due to clamping at the fixed end.

The normal stress distribution in the faces of the sandwich beam is found to be linear across the thickness of the face sheets. This is in conformity with the engineering theory of bending for beams. For beams numbered 1, 3 and 5 , having a nominal face thickness of 1/16 inch ( Figs. 18, 20 and 22 ), the variation of normal stresses across the thickness is small. Therefore, it is a reasonable approximation to say that the normal stresses are uniform in the case of sandwich beams with relatively thin face sheets. However, beams numbered 2 and 4 exhibit a sharp variation of normal stresses across their thickness. One possible reason for this, besides their relatively higher thickness, could be a probable slip at the interface of the core and face sheets. Despite extreme care in maintaining a uniform thickness of cement at the interfaces, few air bubbles could have been locked within the models at the interfaces. Such a situation would lead to a slip at the interface, and a consequent independent action by the faces and core in carrying the applied load. If the faces independently take the bending load, the neutral axis would have been at the mid-plane of the face sheets. Obviously, this is not the case for beams numbered 2 and 4 even though there is a definite slip. It is also observed that the normal stresses in beams having thinner face sheets (# 1, 3 and 5) have a higher magnitude, compared to those in the cases of beams #2 and #4.

The shear stresses in the cores are found to be reasonably uniform in beams numbered 1, 3 and 4. Local effects near the interfaces are pronounced in all the cases. It is therefore concluded that, the approximation to consider a constant shear stress distribution across the core thickness for theoretical investigations, is justified. While performing the experiments, the isoclinics in the core, as well as the isochromatics were observed to be wide bands, rather than well defined sharp fringes. This means that the maximum principal stress difference or the maximum shear stress is a constant in the core. Further, the isoclinic parameter was observed to vary from 43 to 47 degrees. An isoclinic parameter of 45 degrees indicates pure shear and from the observations again, it is justifiable to assume that the core takes up only shear. This is further strengthened by the fact that, bulk of the core material used in engineering practice is of honeycomb construction which is capable of taking only shear.

The relatively large local variations of shear stresses in the cases of beams 2, 3 and 5 may be attributed to possible slips and resultant bending resistance of core and cement in this region. Further, residual stresses were observed in a few instances after unloading the beams. This is indicative of a slip between the faces and core, which results in locking some stresses. The orders of isochromatic fringes, which were observed to be wide bands in the core, were determined at 0.025" intervals using the uniform field compensator. Errors in determining the exact order of such fringes with a visual judgment of minimum light intensity alone are possible. For all practical purposes, the Tardy compensation technique would not have been sensitive to such small differences in fringe orders in the core. It was in view of this fact that, this method was not used in identifying the fringe orders.

Table II shows a cross-check for the computed internal stresses from calculations of moment and shear balance. The differences observed are probably due to load concentrations at discrete points and partial losses in load transmission.

The transverse deformations were measured at different stations along the length of the beams. The vernier micrometer attached to the table of the polariscope was used for this purpose. The values are plotted in figures 23 to 27, against the theoretical curve obtained by finite element method. A reasonably good agreement is observed between the experimental results and theoretical prediction. In the theoretical investigation, the compression of the core was neglected and the transverse deformation was assumed to be constant across the depth of the beam. Core compressions were computed from experimental data and are given as a percentage of the maximum normal stresses, in Table II. The measurement of transverse deformations close to the free end of the beam, was not possible because of the images of the beams going out of the view in the screen. The beam dimensions, as discussed in the chapter on experimentation, were dictated by the table movements of the polariscope and manufacturing facility. An attempt was made to keep the beams slender, so that they do not approach the dimensions of a deep beam. A length to depth ratio of 5.25 was kept as a limiting value. The axial deformations were of a small order and could not be accurately determined using this instrument.

Figures 28 to 32 correspond to the deformation pattern obtained for different types of load conditions, using the Finite Element Method. A length to depth ratio of 10:1 is considered and the deformation patterns are plotted for three different face thickness to overall depth ratios. The face sheet material is taken to be aluminum, which is frequently used as the skin material. A shear modulus to Young's modulus ratio of $10^{-3}$ is considered between the core and face sheet material. Such a ratio is often used in structural sandwiches, having honeycomb cores.

The deformation curves are plotted for the following five load conditions:

(i) Transverse loading of uniform intensity.( Fig.28 )

(ii) Transverse and axial loading, with axial load equal to half the intensity of transverse loading. ( Fig.29 )

(iii) Transverse and axial loading of equal intensity. ( Fig.30 )

(iv) Transverse loading with linear axial loading having a maximum intensity of half the transverse load intensity. ( Fig.31 )

(v) Transverse loading and linear axial loading having a maximum intensity equal to that of the transverse load. ( Fig.32 )

These figures indicate an increase in transverse deformation with decreasing f/H ratios. This is because of a lower bending rigidity with decreasing face thickness. The axial deformation shows a rapid increase near the fixed end of the beam indicating high strain rate in this region. Again, axial deformation is found to increase with decreasing f/H ratios.

The magnitudes of transverse deformation are observed to decrease with increasing axial loading. This is because of the axial load producing a moment which is opposite to the sign of the bending moment. The axial deformation in these cases is observed to increase with the intensity of the axial load. However, the maximum axial deformation is found to be within 4% of the maximum transverse deformation. Table III gives a comparative idea of the ratio of the maximum axial deformation to the maximum transverse deformation for different intensities of loading ( marked as Type I, Type II etc. ) and face thickness to depth ratios.

In this analysis, the boundary conditions derived in Section II.3, and represented by equations (2.17) and (2.18) cannot be applied. These equations involve the quantity $w_{xxx}$ which is not a degree of freedom for this problem. A possible reason for the change in the slope of the deformation curve near the free end of the beam could be the violation of this boundary condition. Because of this reason, the total potential energy of the beam is not actually minimized and the configuration assumed by the beam in such a situation is not the one satisfying the equilibrium conditions.

TABLE I

| Beam No. | f (in) | h (in) | d (in) |
|---|---|---|---|
| 1 | 0.065 | 0.871 | 0.254 |
| 2 | 0.124 | 0.747 | 0.255 |
| 3 | 0.063 | 0.754 | 0.254 |
| 4 | 0.124 | 0.635 | 0.255 |
| 5 | 0.065 | 0.632 | 0.254 |

TABLE II

| Beam No. | Bending Moment ( lb-in ) | | Shear Force ( lb ) | | Core Compression |
|---|---|---|---|---|---|
| | External | Internal | External | Internal | ( % ) |
| 1 | 3.445 | 4.144 | 1.499 | 1.496 | 1.540 |
| 2 | 3.445 | 3.580 | 1.499 | 1.163 | 0.973 |
| 3 | 3.445 | 3.911 | 1.499 | 1.346 | 2.230 |
| 4 | 3.445 | 3.835 | 1.499 | 0.902 | 1.120 |
| 5 | 3.445 | 3.446 | 1.499 | 1.434 | 0.389 |

TABLE III

| Load Type | f/H | $\frac{u_{max}}{w_{max}}$ % |
|---|---|---|
| | 0.05 | 3.21 |
| I | 0.10 | 2.11 |
| | 0.15 | 1.58 |
| | 0.05 | 3.39 |
| II | 0.10 | 2.21 |
| | 0.15 | 1.62 |
| | 0.05 | 3.33 |
| III | 0.10 | 2.18 |
| | 0.15 | 1.61 |
| | 0.05 | 3.58 |
| IV | 0.10 | 2.31 |
| | 0.15 | 1.65 |
| | 0.05 | 3.46 |
| V | 0.10 | 2.24 |
| | 0.15 | 1.63 |

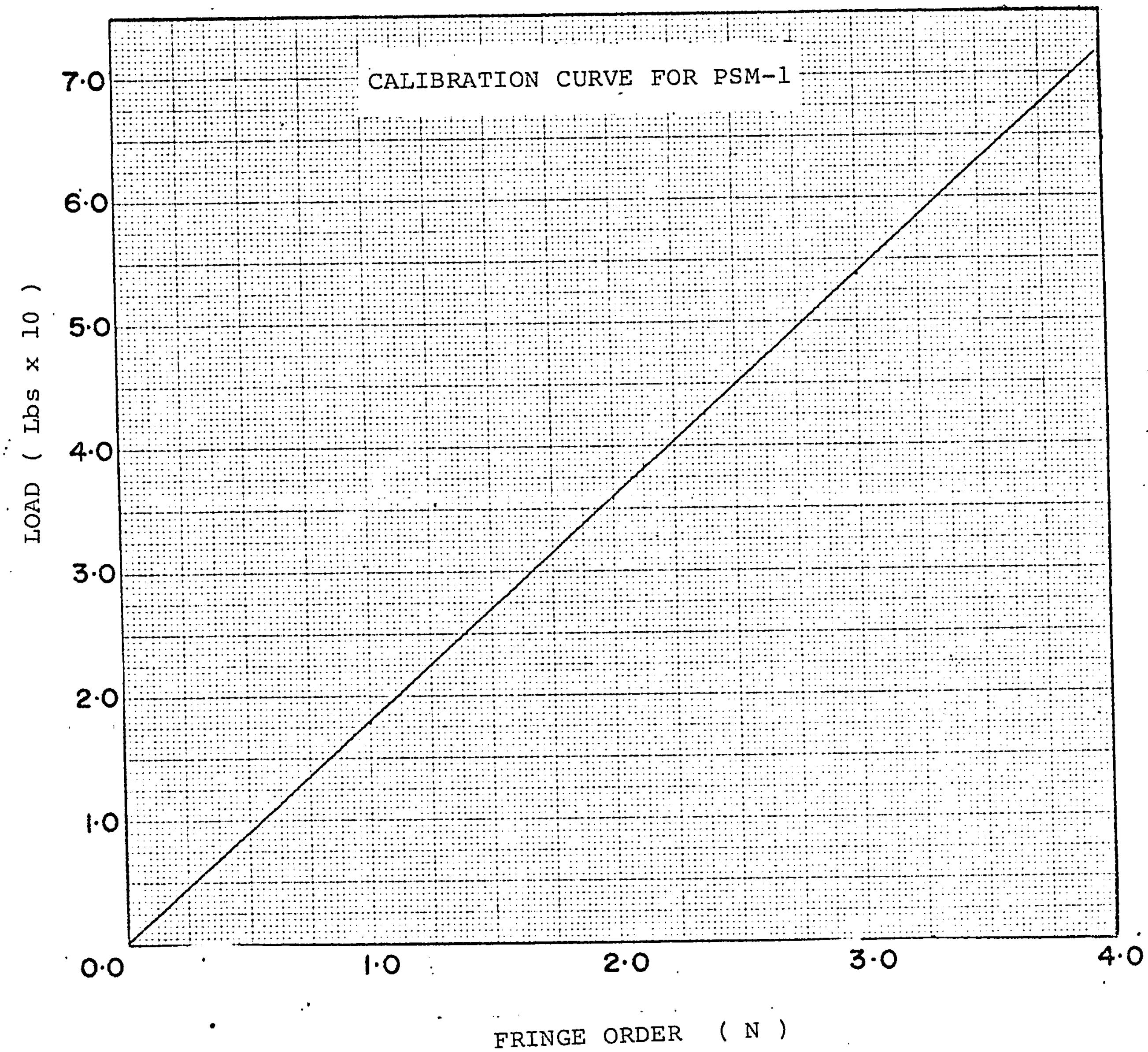
CALIBRATION CURVE FOR PSM-1
7·0
6·0
5·0
4·0
3·0
2·0
1·0
0·0
1·0
2·0
3·0
4·0
LOAD ( Lbs x 10 )
FRINGE ORDER ( N )

Fig.13

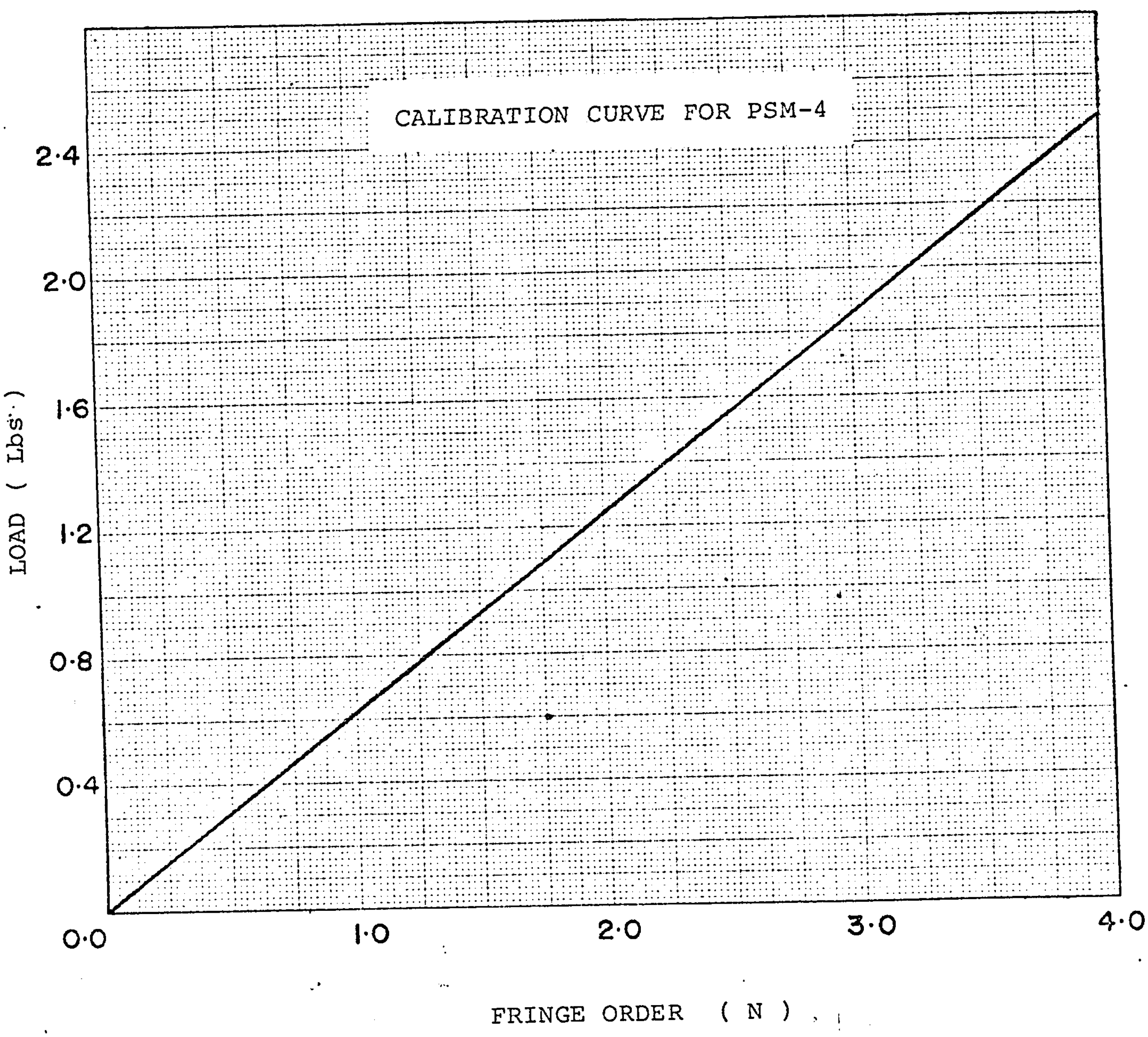
CALIBRATION CURVE FOR PSM-4
2·4
2·0
1·6
1·2
0·8
0·4
LOAD ( Lbs )
0·0
1·0
2·0
3·0
4·0
FRINGE ORDER ( N )

Fig.14

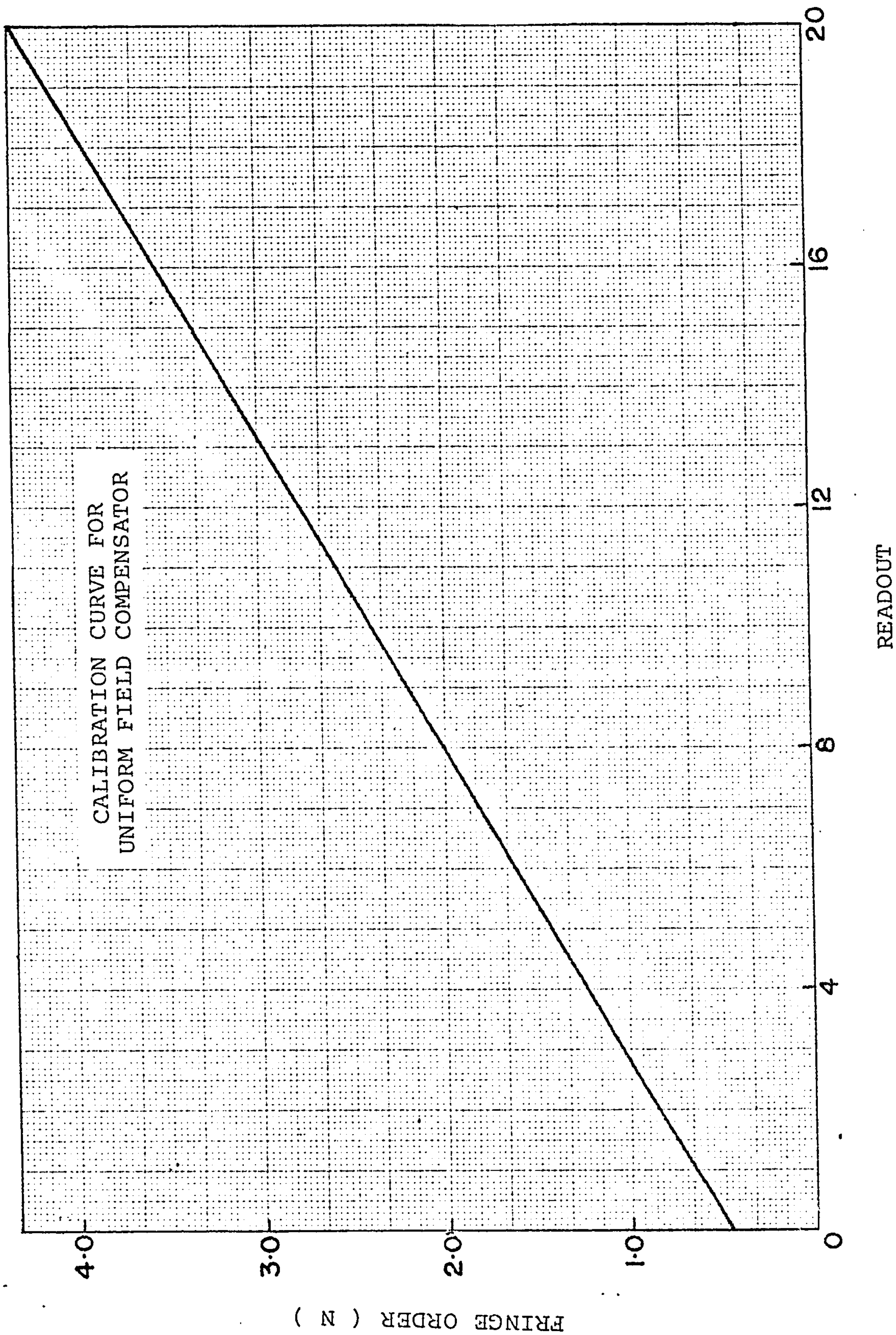
CALIBRATION CURVE FOR
UNIFORM FIELD COMPENSATOR
FRINGE ORDER ( N )
4·0
3·0
2·0
1·0
0
4
8
12
16
20
READOUT

Fig.15

## TENSILE TEST ON PSM-1

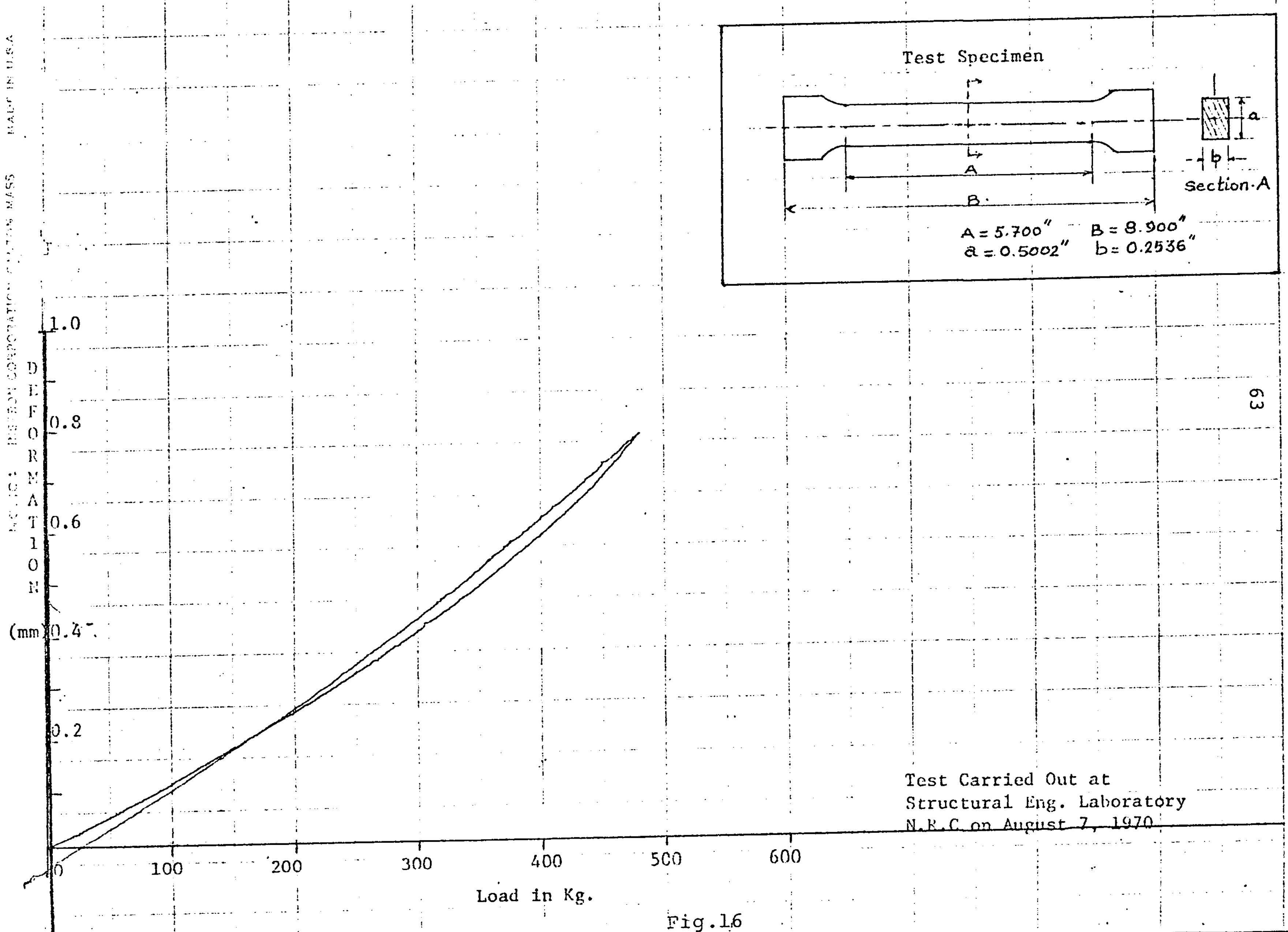


Fig.16

Fig.17 TENSILE TEST ON PSM-1

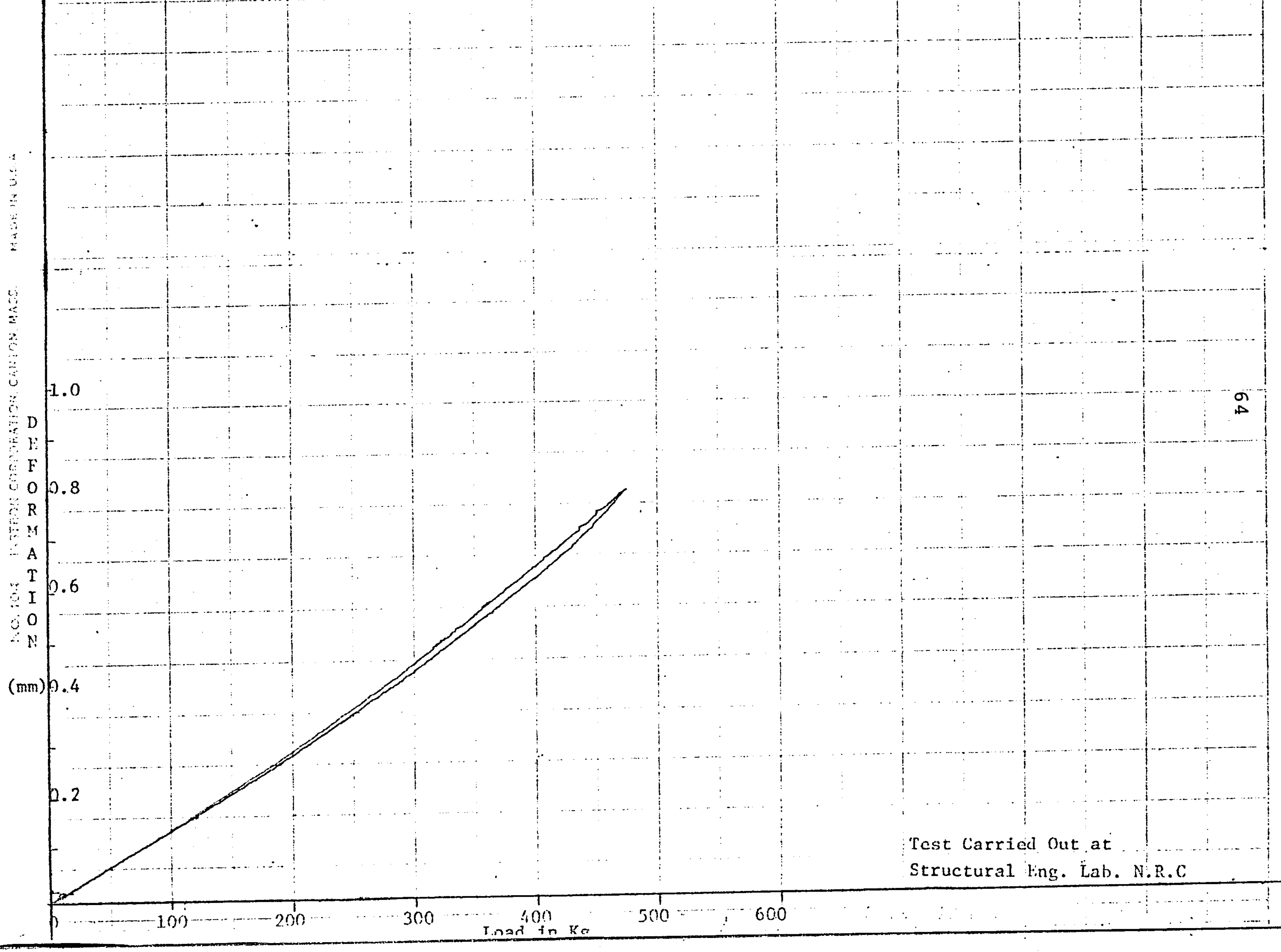

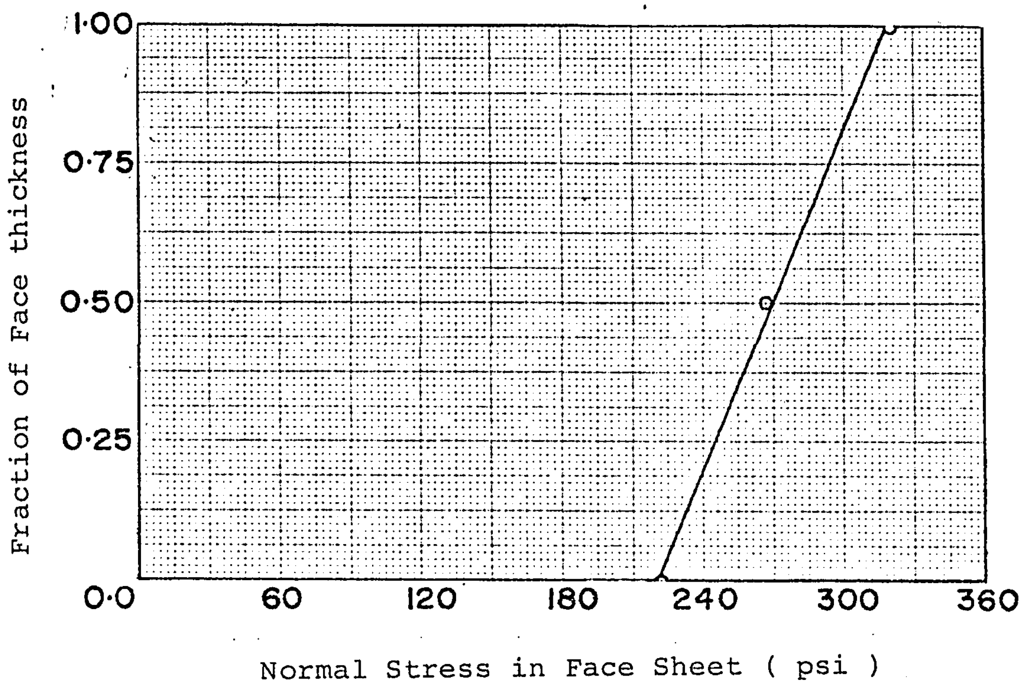


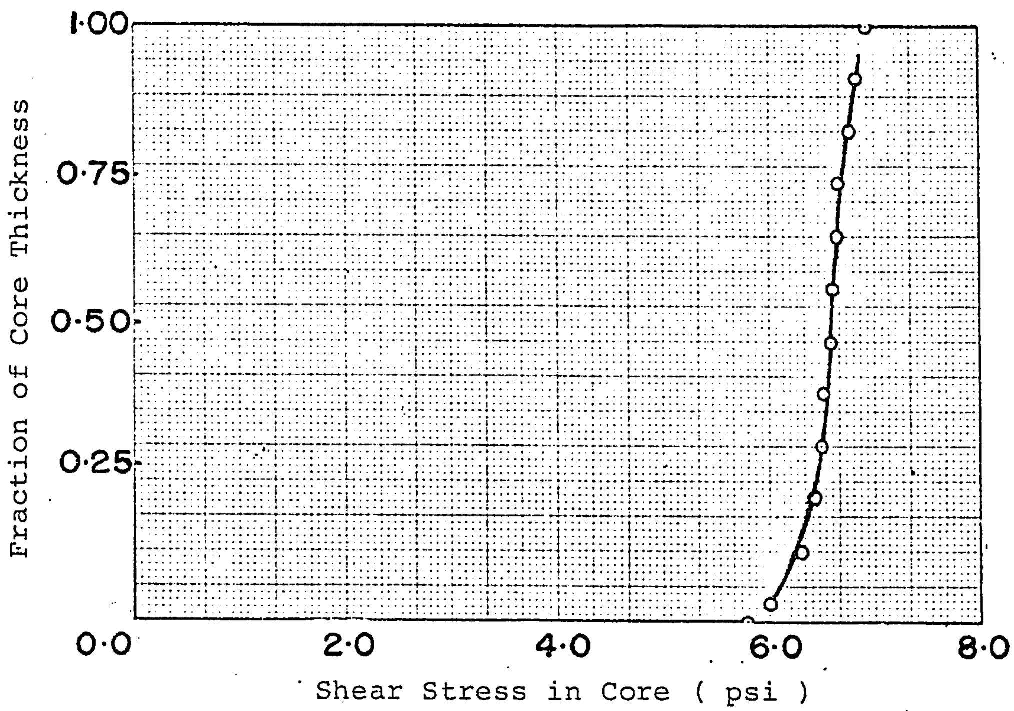


Fig.18 Stress Distribution in Beam 1

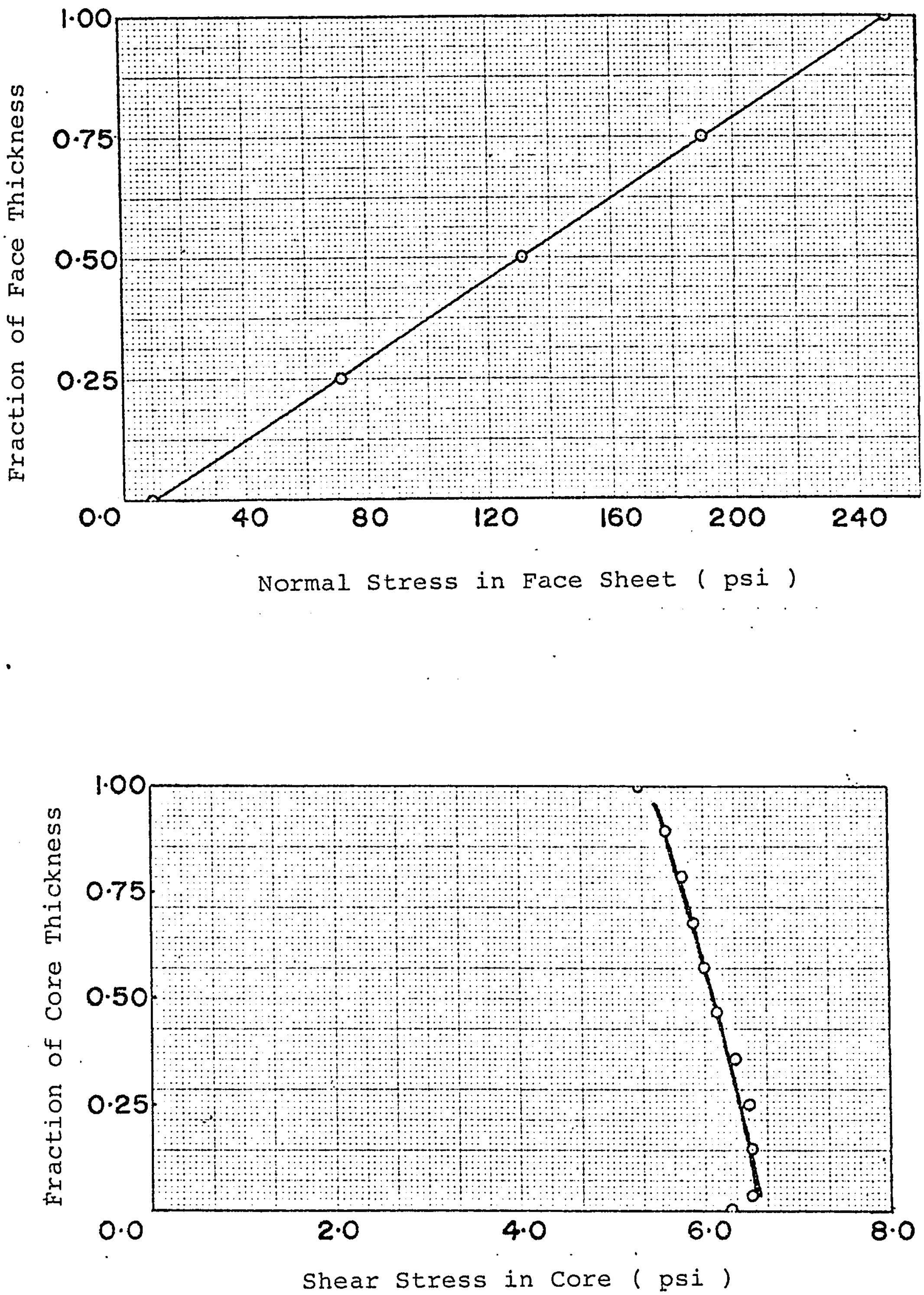


Fig. 19 Stress Distribution in Beam 2

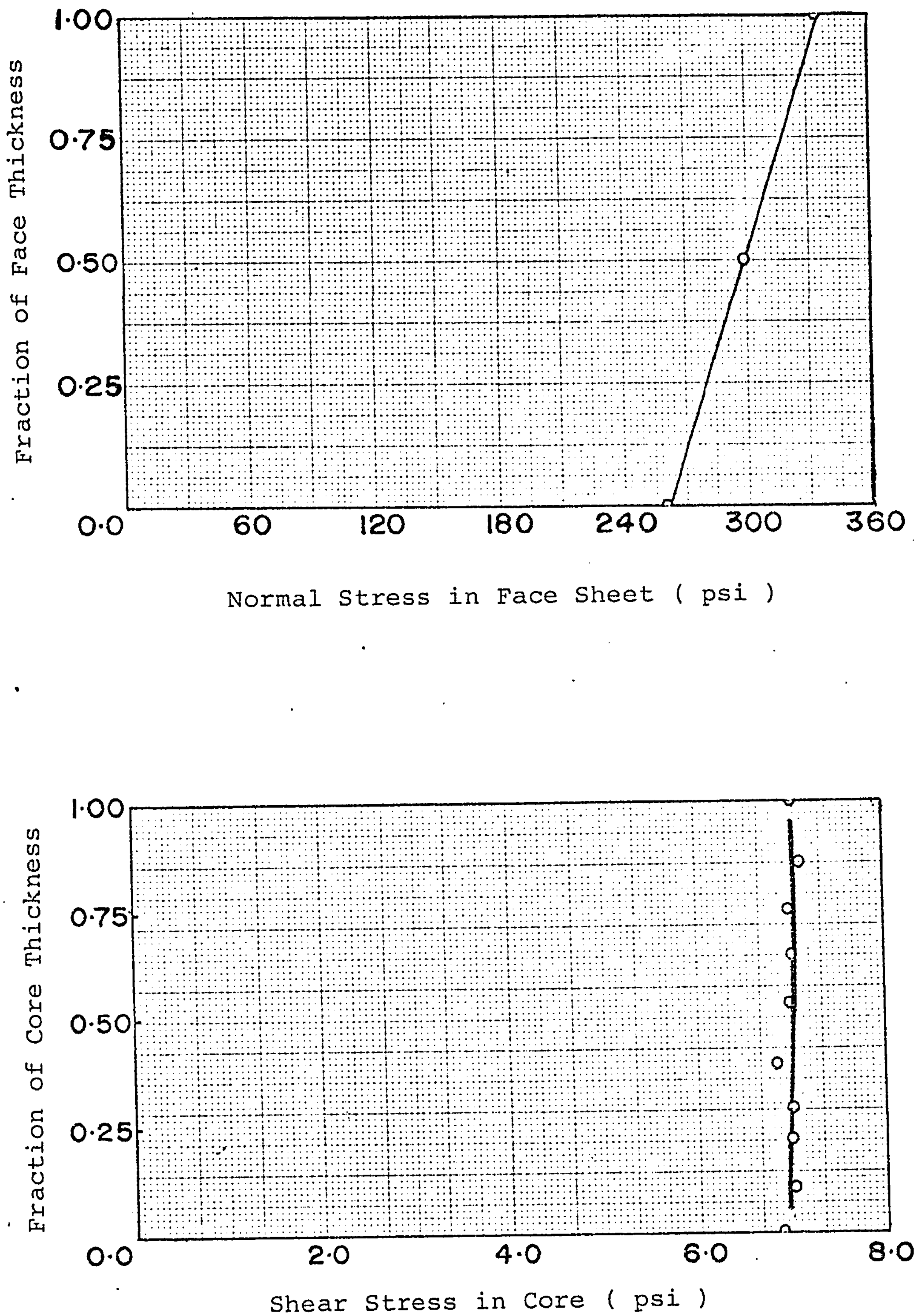


Fig.20 Stress Distribution in Beam 3

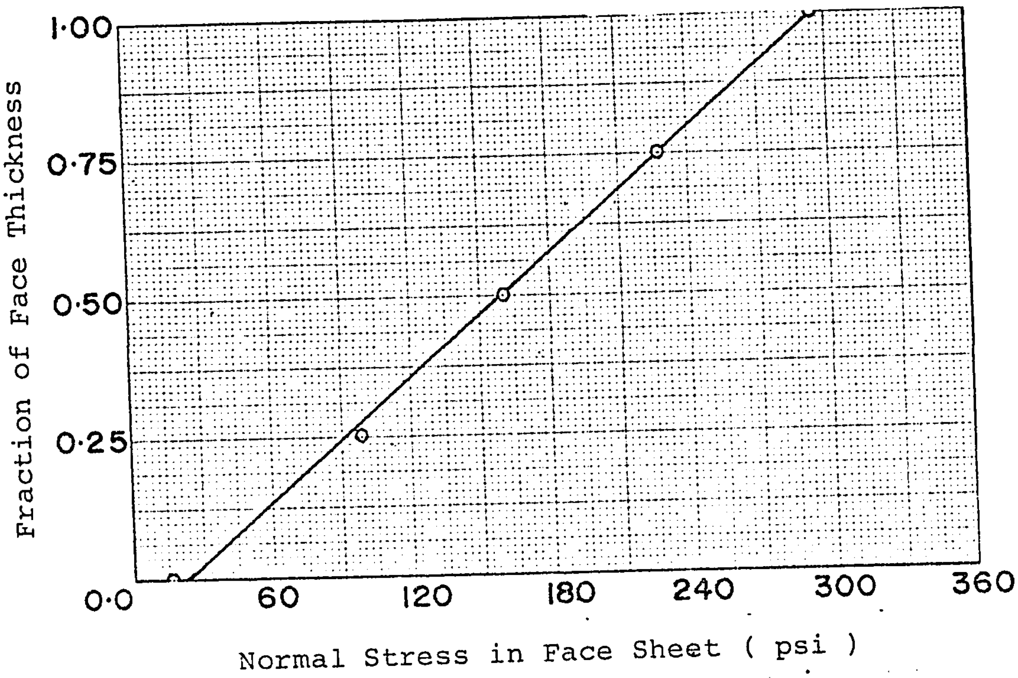


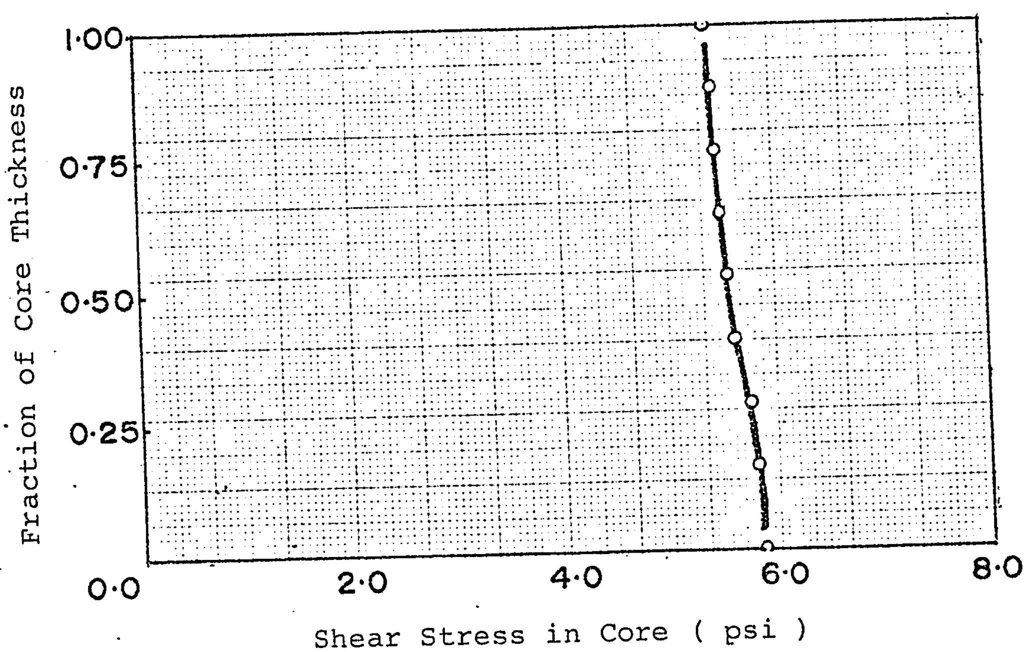


Fig.21 Stress Distribution in Beam 4

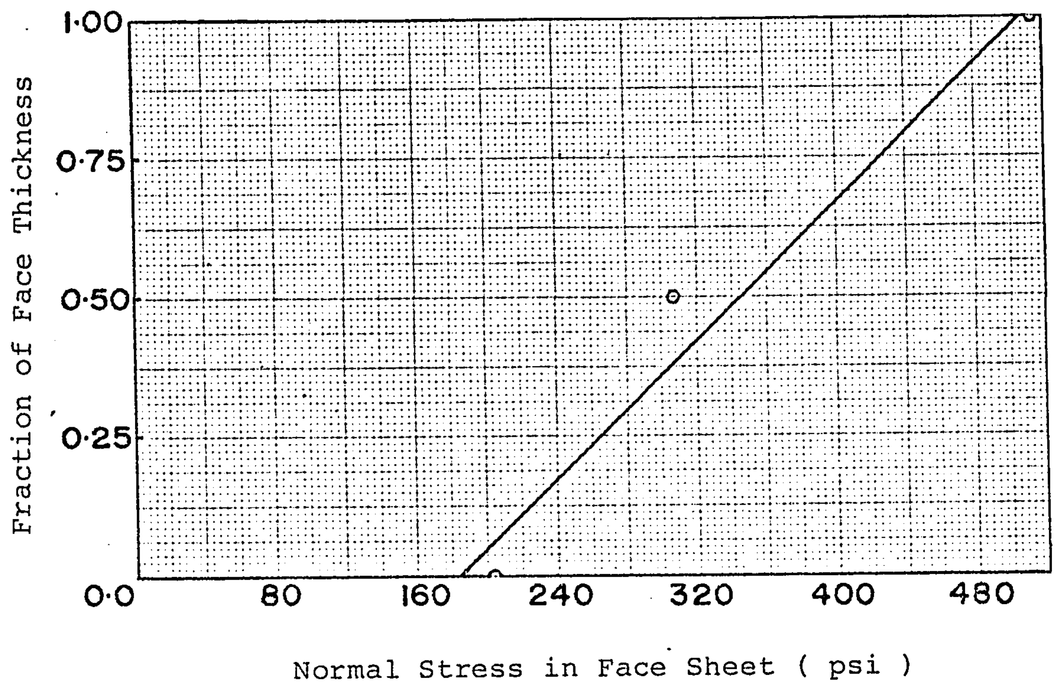


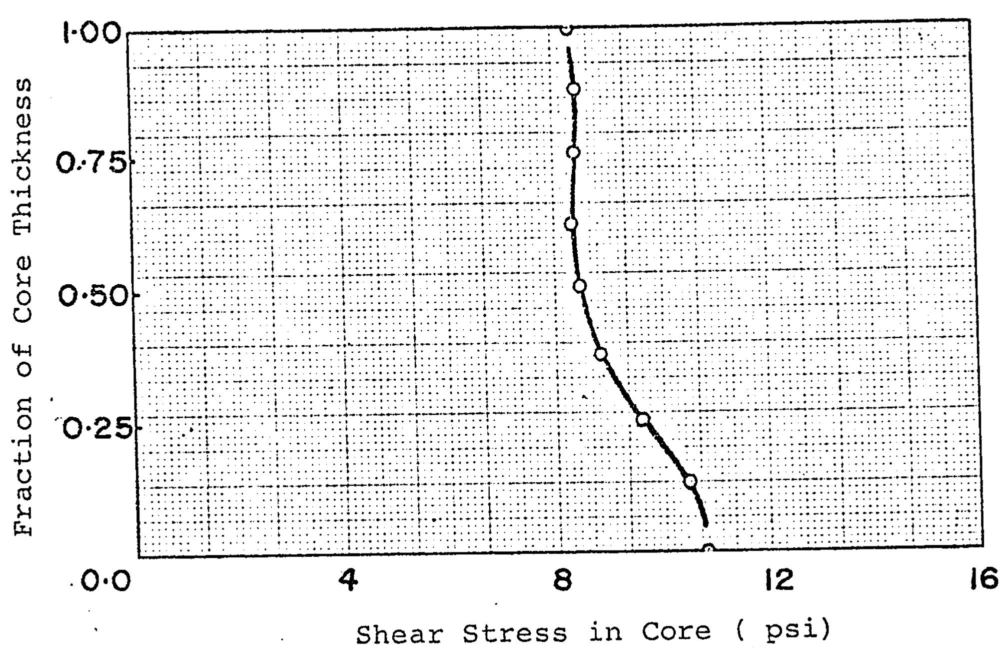


Fig.22 Stress Distribution in Beam 5

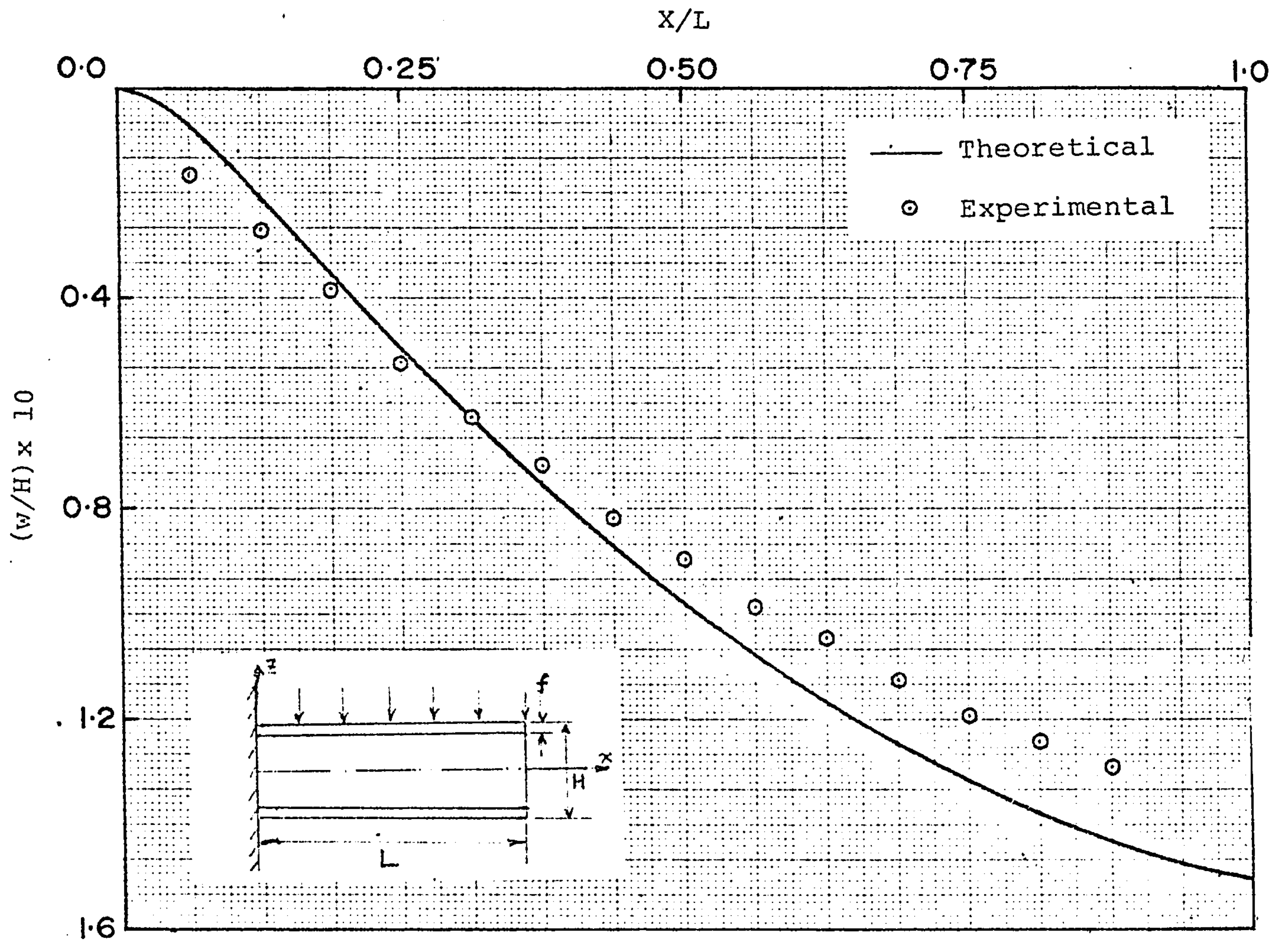


Fig.23 Transverse Deformation in Beam 1

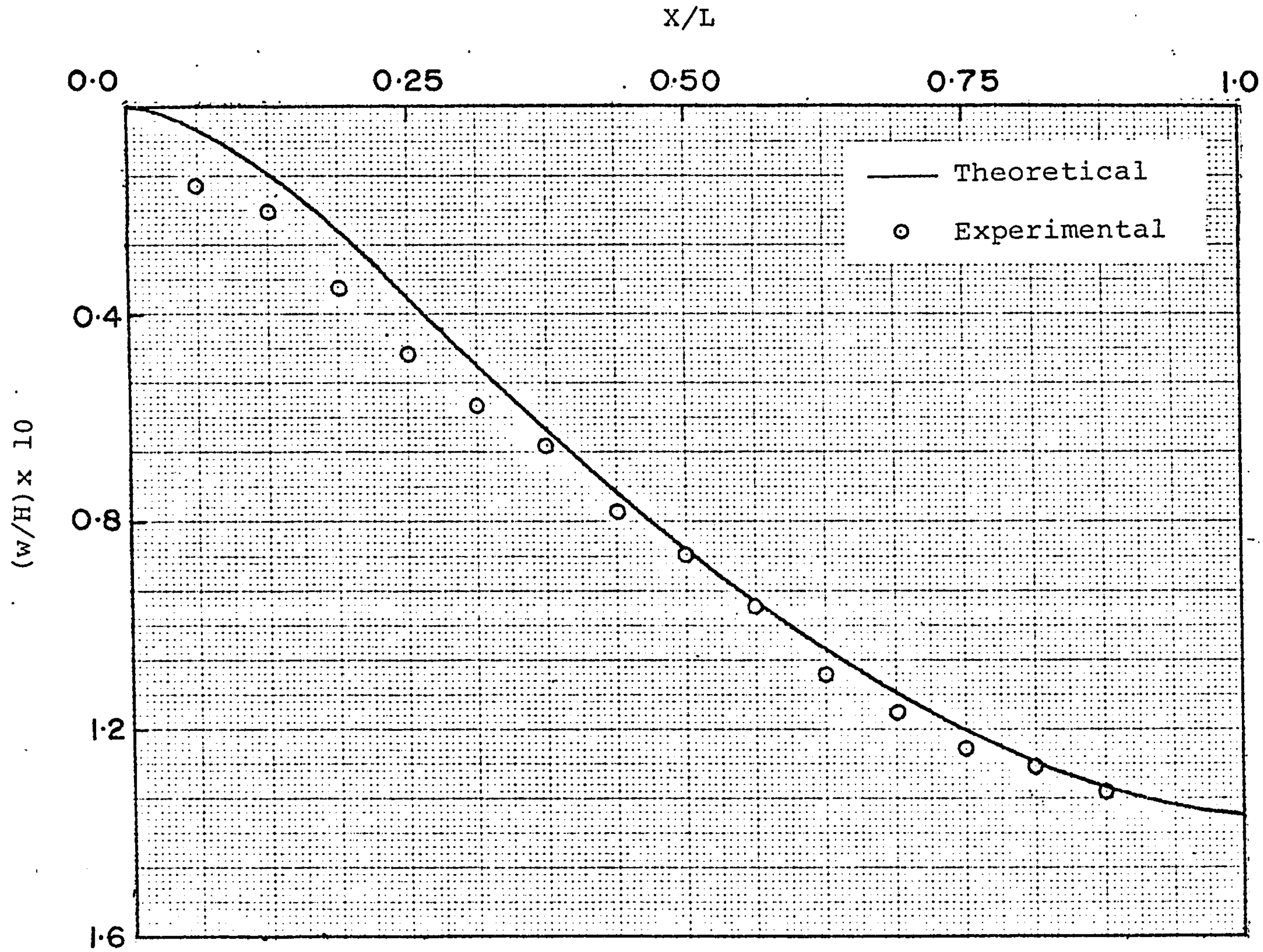


Fig.24 Transverse Deformation in Beam 2

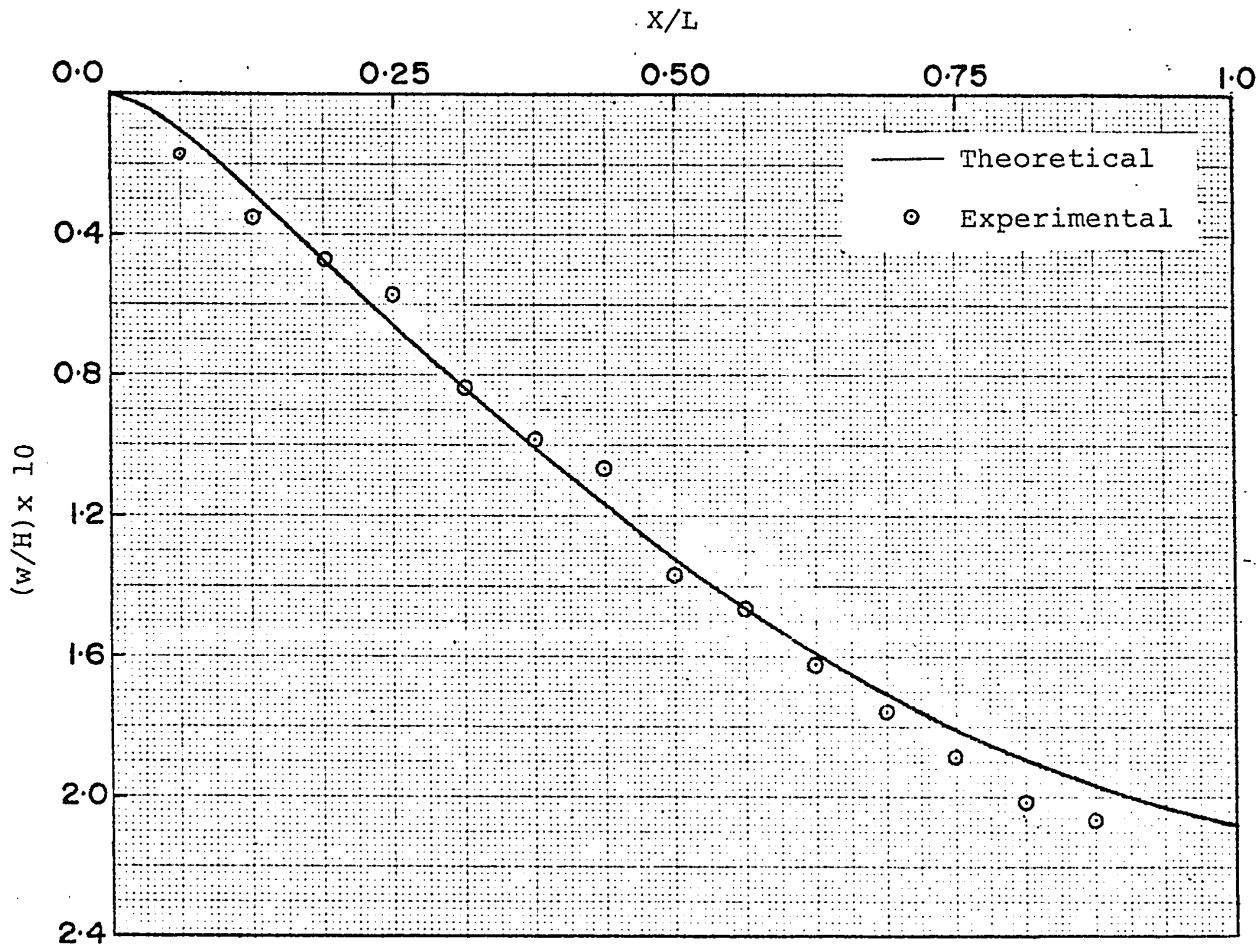


Fig.25 Transverse Deformation in Beam 3

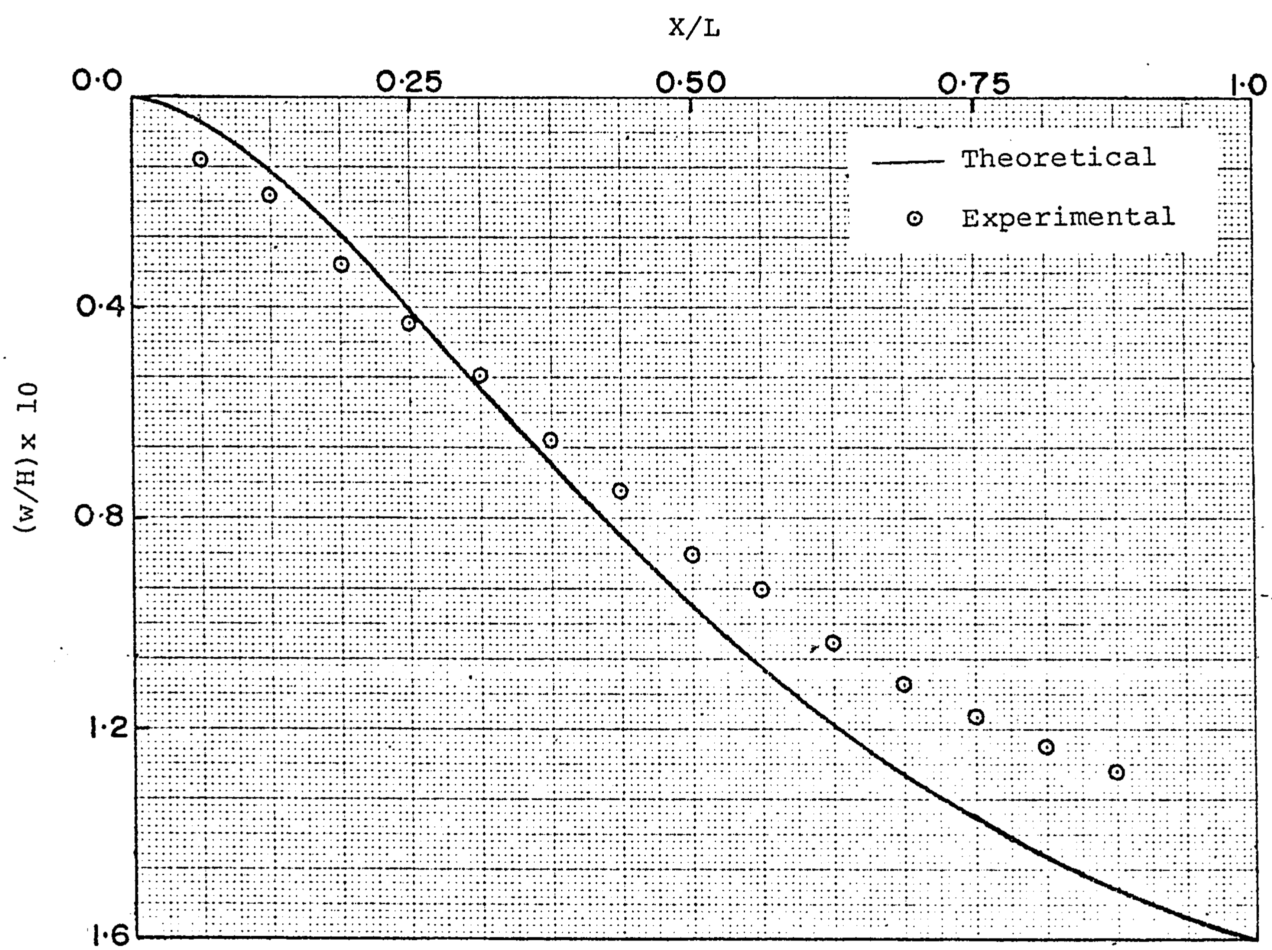


Fig.26 Transverse Deformation in Beam 4

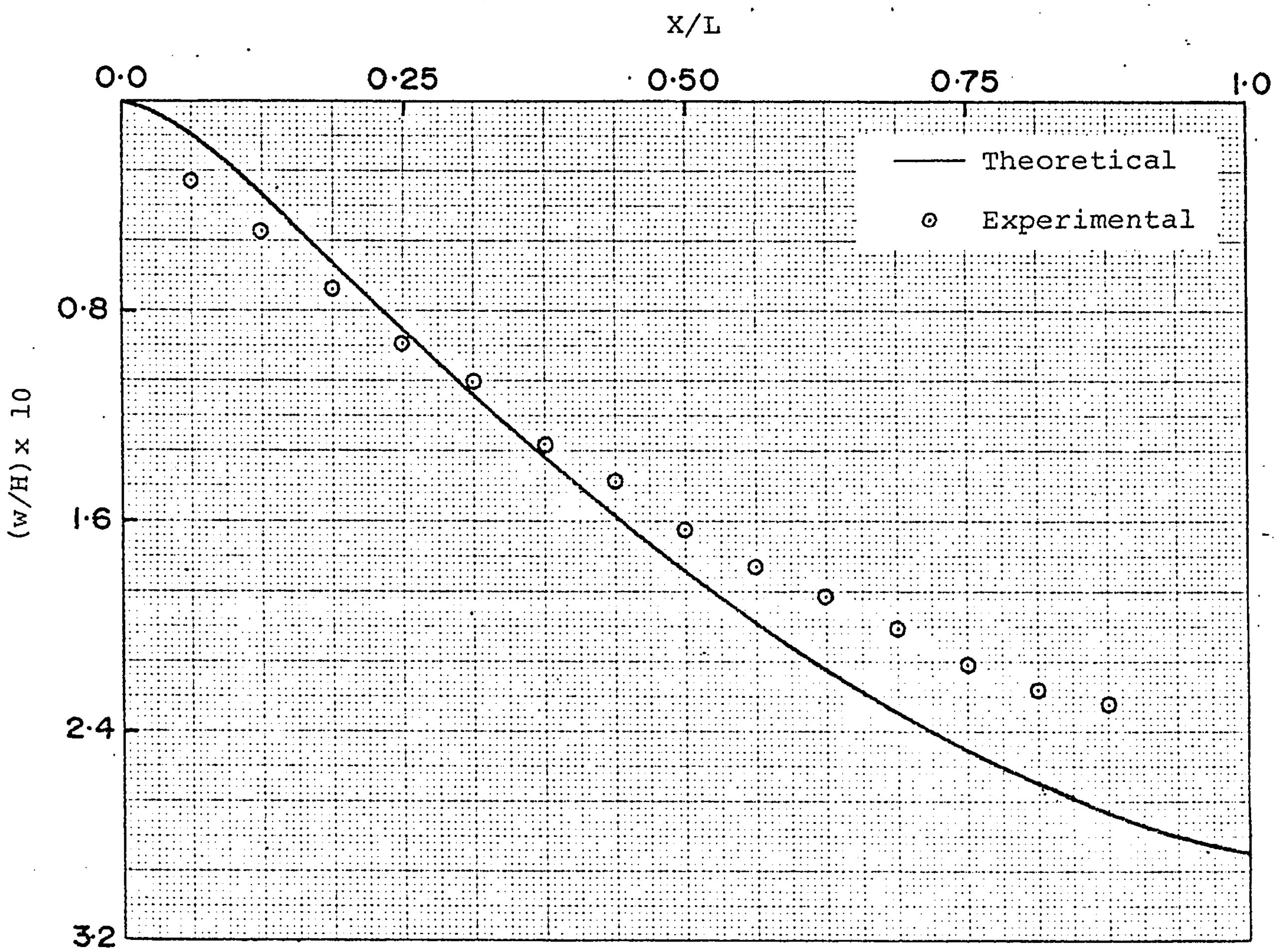


Fig.27 Transverse Deformation in Beam 5

Fig.28

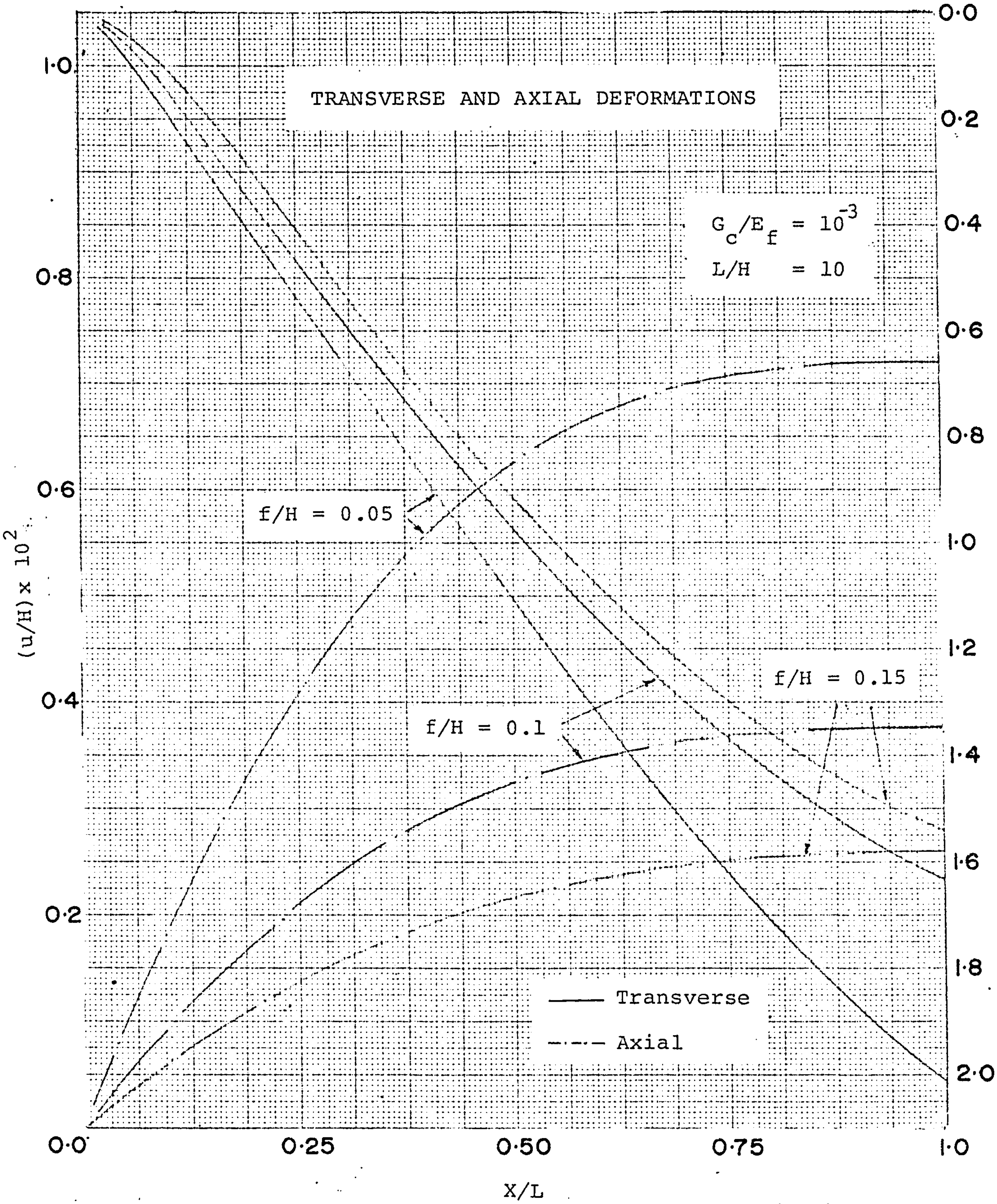


Load Type I — $F_a = 0$

Fig.29

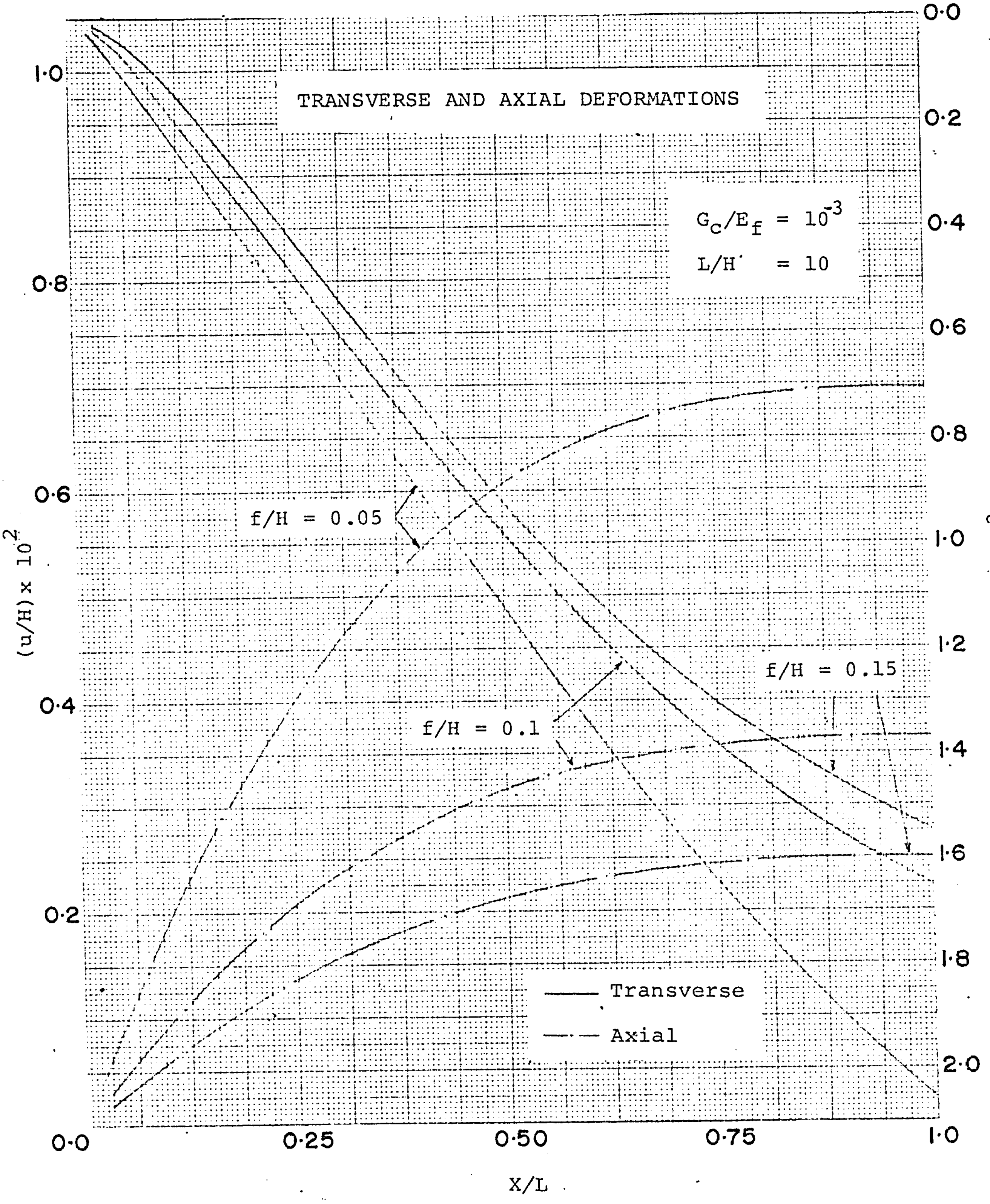


Load Type II — $F_a = 0.5 F_t$

Fig.30

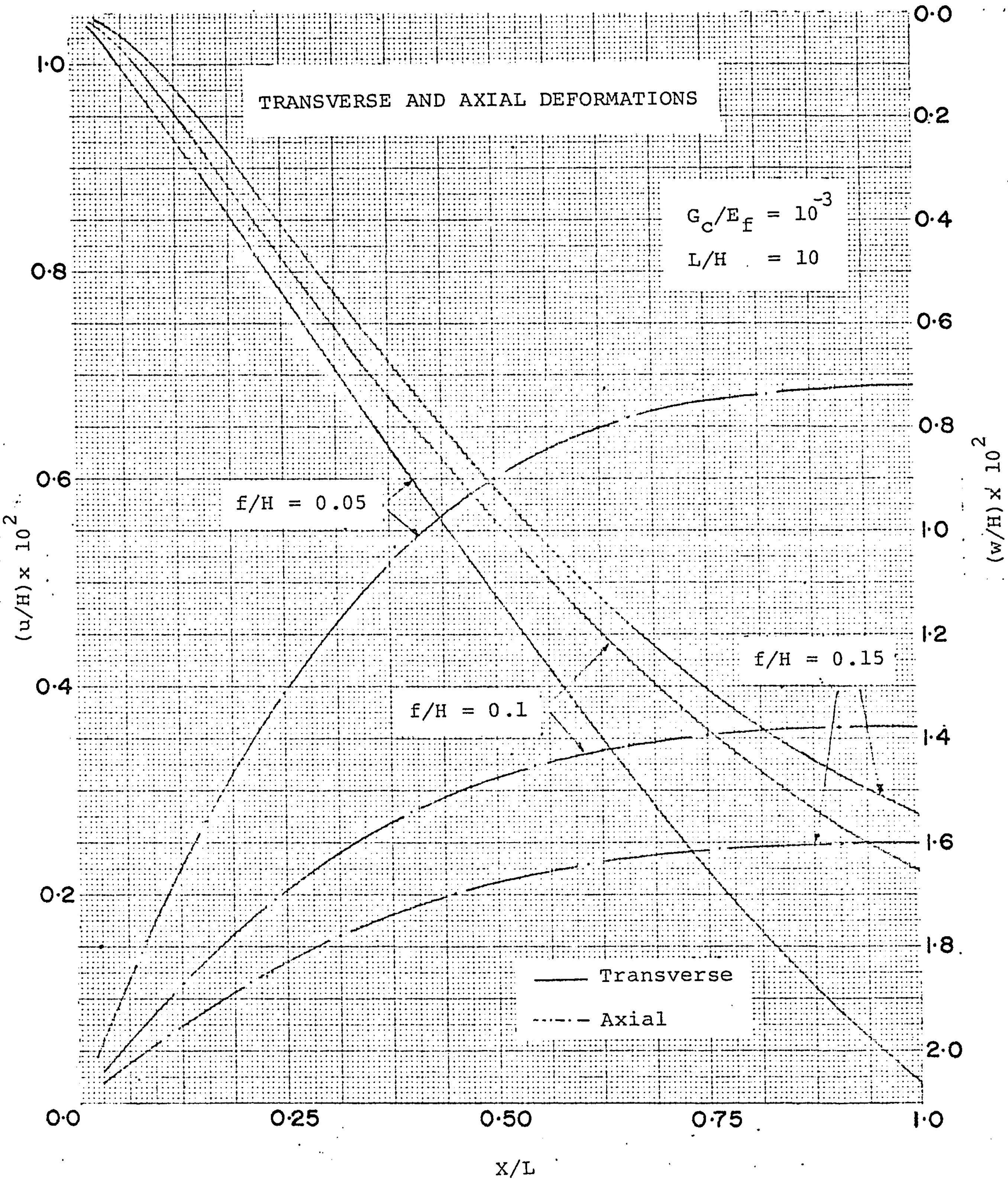


Load Type III — $F_a = 0.5 \frac{X}{L} F_t$

Fig.31

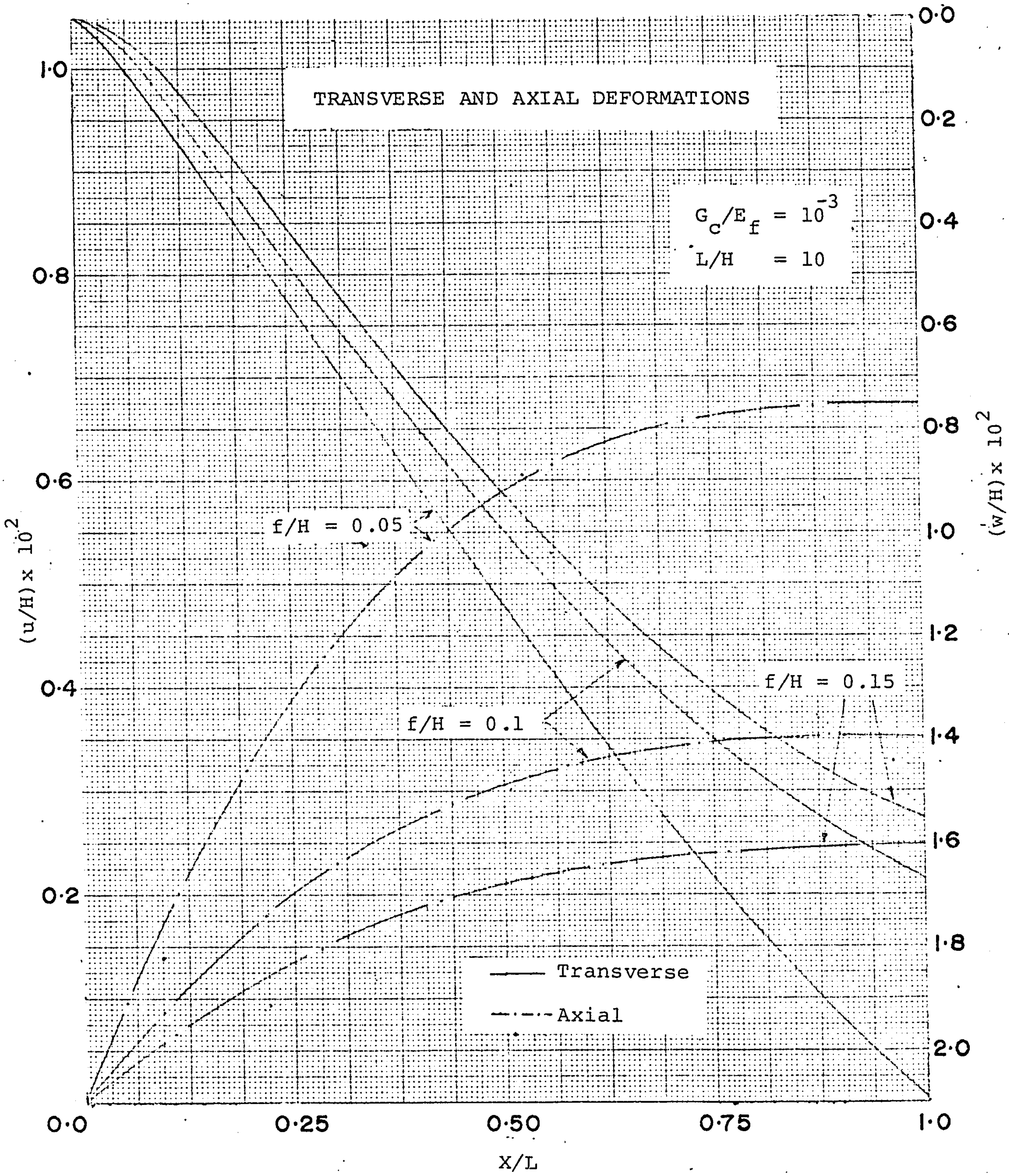


Load Type IV — $F_a = F_t$

Fig.32

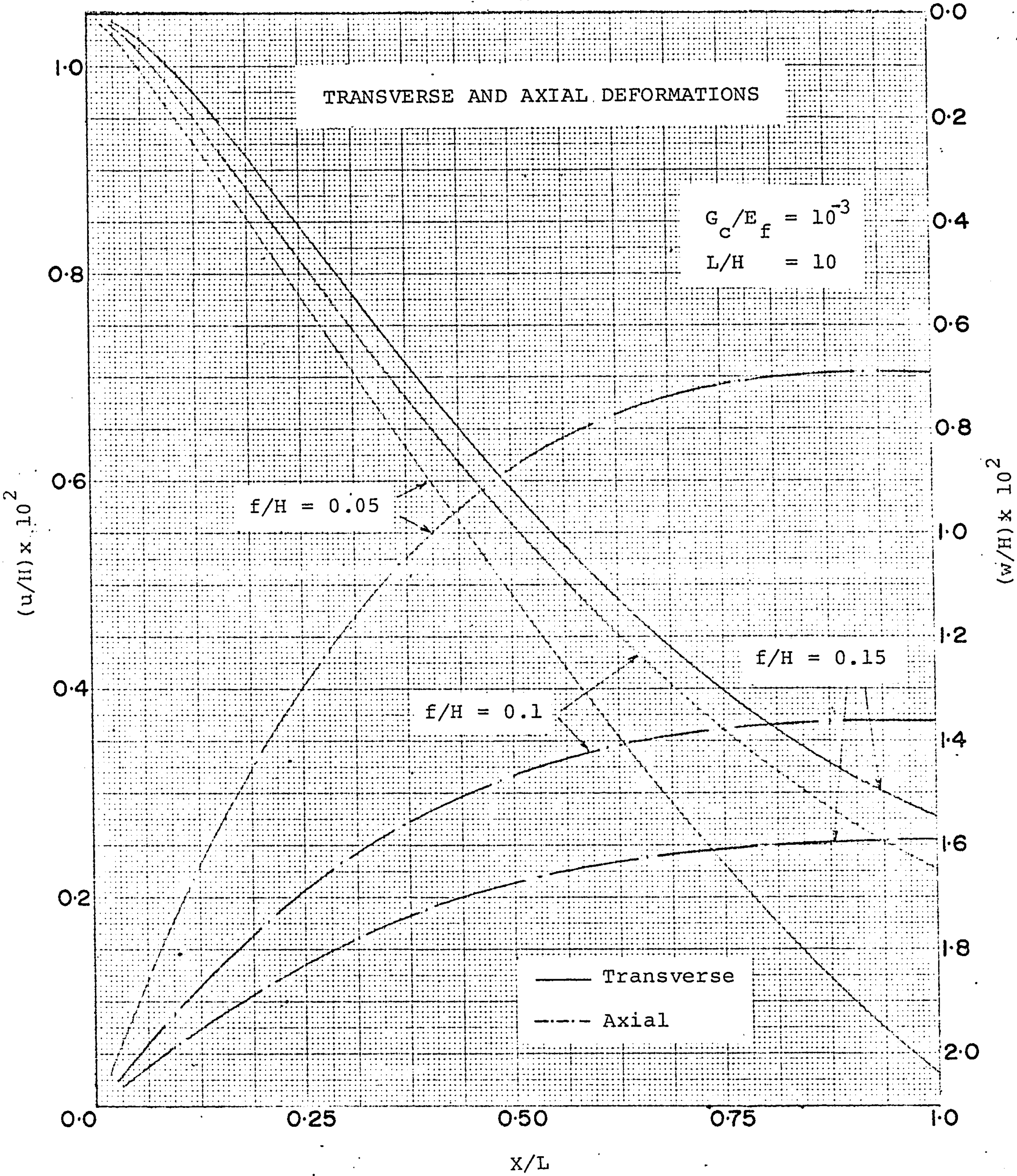


Load Type V — $F_a = \frac{x}{L} F_t$

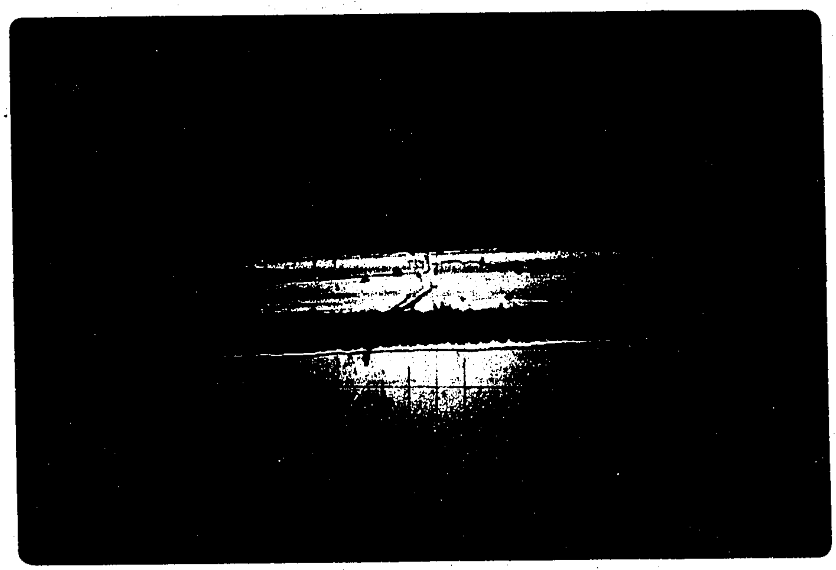

Fig.33  Isochromatics in Beam 1

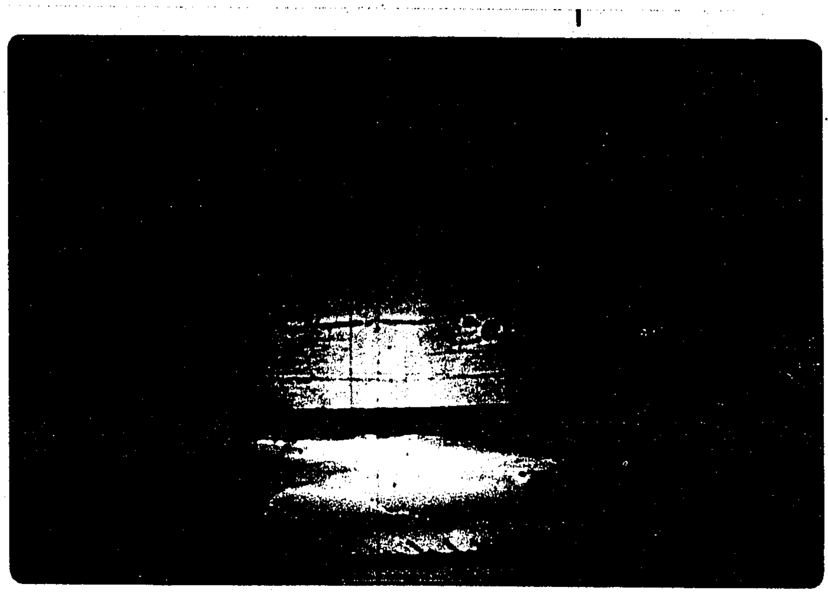

Fig.34  Isochromatics in Beam 4

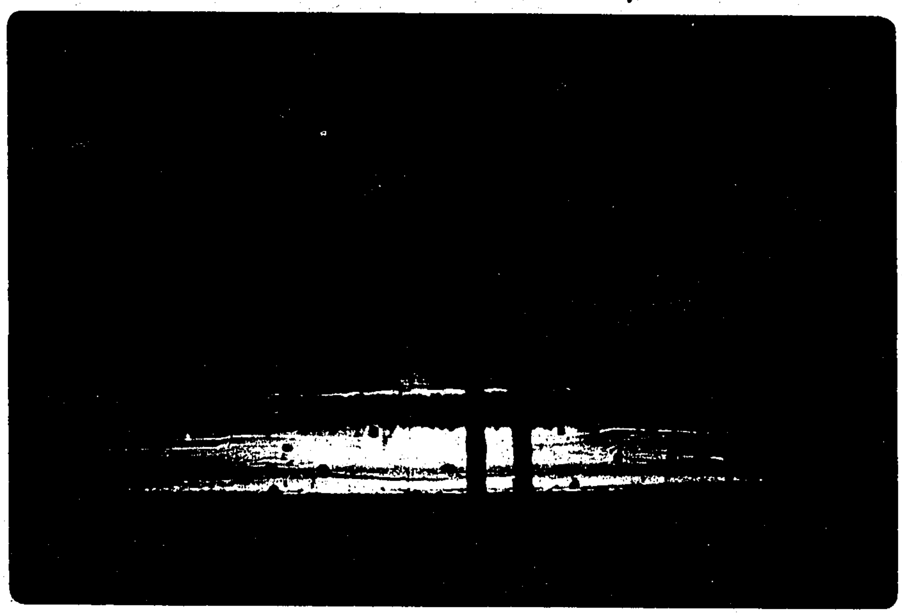

Fig.35  $45^{0}$ Degree Isoclinic in Beam 3

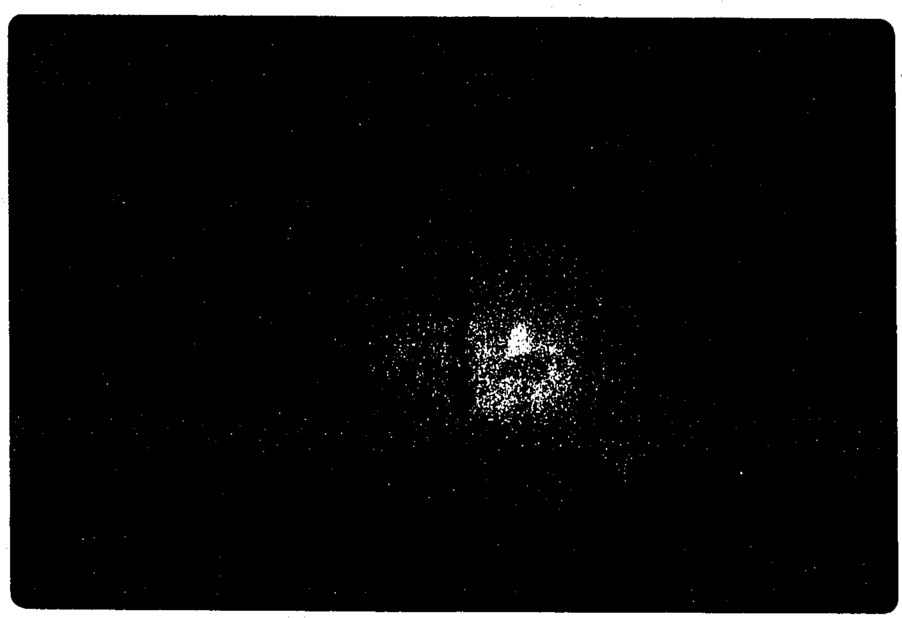

Fig.36  Isochromatics in the Core of Beam 2

# VI APPENDIX

1. Shear difference method

This is a numerical procedure used to determine the principal stresses at the interior points in the model. The method is based on equations of equilibrium, which in plane stress problems in the absence of body forces are,

$$\frac{\partial \sigma_{xx}}{\partial x} + \frac{\partial \tau_{xy}}{\partial y} = 0 \qquad \text{(i)}$$

$$\frac{\partial \tau_{xy}}{\partial x} + \frac{\partial \sigma_{yy}}{\partial y} = 0 \qquad \text{(ii)}$$

Equation (i) can be integrated along x, given in Fig.12 as follows.

$$\frac{\partial \sigma_{xx}}{\partial x} dx = - \frac{\partial \tau_{xy}}{\partial y} dx \qquad \text{(iii)}$$

The above equation can be represented by finite difference method as,

$$\frac{\partial \sigma_{xx}}{\partial x} dx = \sigma_{xx}\Big|_{x_1} - \sigma_{xx}\Big|_{x_0} = - \frac{\Delta \tau_{xy}}{\Delta y}\Big|_{\frac{(x_0+x_1)}{2}} \Delta x \qquad \text{(iv)}$$

where $x_0$, $x_1$, $x_2$ are positions along x axis. $\Delta x$ and $\Delta y$ are finite intervals along x and y axes as defined in the figure. For a particular case of equal spacing along x and y, equation (iii) reduces to,

$$\sigma_{xx}\Big|_{x_1} = \sigma_{xx}\Big|_{x_0} - \Delta \tau_{xy}\Big|_{\frac{(x_0+x_1)}{2}}$$

The value $\sigma_{xx}\big|_{x_0}$ is directly obtained from isochromatic data, as $x_0$ is on the free boundary. The value of $\Delta\tau$ can be computed from isoclinic and isochromatic data. Hence it is possible to determine at an interior point $x_1$. By proceeding in steps along x, the value of $\sigma$ can be determined along the entire length of line OP, from the following recurrence equations.

$$\sigma_{xx}\big|_{x_2} = \sigma_{xx}\big|_{x_1} - \Delta\tau_{xy}\big|_{\frac{(x_1+x_2)}{2}}$$

$$\sigma_{xx}\big|_{x_3} = \sigma_{xx}\big|_{x_2} - \Delta\tau_{xy}\big|_{\frac{(x_2+x_3)}{2}}$$

$$\sigma_{xx}\big|_{x_4} = \sigma_{xx}\big|_{x_3} - \Delta\tau_{xy}\big|_{\frac{(x_3+x_4)}{2}}$$

This procedure is repeated along the lines AB and CD. The stress $\sigma$ can now be computed from the following relations.

$$\sigma_{yy} = \sigma_{xx} - (\sigma_1 - \sigma_2)\,\mathrm{Cos}\,2\theta$$

or

$$\sigma_{yy} = \sigma_{xx} - \frac{Nf}{h}\,\mathrm{Cos}\,2\theta$$

where N and $\theta$ are data from the photoelastic experiment and f and h are the Stress Optic Constant and thickness of the model. The principal stresses can be easily computed from the following relations.

$$\sigma_1 = \tfrac{1}{2}(\sigma_{xx} + \sigma_{yy} + Nf/h)$$

$$\sigma_2 = \tfrac{1}{2}(\sigma_{xx} + \sigma_{yy} - Nf/h)$$

This method employs only isoclinic and isochromatic data, and can be used to separate stresses along any arbitrary line OP. The errors in this procedure are cumulative, as it is numerical integration process. Therefore, this method demands accurate observation of input data, at close intervals.

PROGRAM LISTINGS

```
FORTRAN IV G LEVEL  18              MAIN              DATE = 70245          11/03/59

                C       ----------------------------------------------------------------
                C
                C       SHEAR - DIFFERENCE METHOD FOR SEPERATION OF STRESSES
                C
                C       REFEREENCE: EXPERIMENTAL STRESS ANALYSIS - DALLY J.W. & RILEY W.F.
                C       MCGRAW - HILL, (1965) , PP. 236-238.
                C
                C       ----------------------------------------------------------------
                C
                C       NF    - NUMBER OF POINTS IN FACE SHEET
                C       NC    - NUMBER OF POINTS IN CORE
                C       CF    - CALIBRATION FACTOR OF UNIFORM FIELD COMPENSATOR
                C       C1    - STRESS OPTIC COEFFICIENT OF FACE MATERIAL
                C       C2    - STRESS OPTIC COEFFICIENT OF CORE MATERIAL
                C       DELX  - STEP SIZE IN X DIRECTION
                C       DELY  - STEP SIZE IN Y DIRECTION
                C       H     - THICKNESS OF MODEL
                C       THETA, THETA1, THETA2 - ISOCLINIC PARAMETER ALONG OX, AB, AND CD
                C       RESPLY.
                C       AN, AN1, AN2  - INTEGRAL PART OF FRINGE ORDERS ALONG OX, AB, AND
                C       CD RESPLY.
                C       ANN, ANN1, ANN2 - FRACTIONAL PART OF FRINGE ORDERS ALONG OX, AB
                C       AND CD RESPLY.
                C       PXX, PYY AND TXY - NORMAL STRESSES ALONG X AND Y AXES, AND
                C       SHEAR STRESSES IN XY PLANE
                C
                C
 0001                   DIMENSION PXX(40),PYY(40),TAB(40),TCD(40),TEF(40),P1(40),P2(40)
                C
                C       CLEAR ARRAYS
                C
 0002                   DO 25 I=1,40
 0003                   PXX(I)=0.
 0004                   PYY(I)=0.
 0005                   TAB(I)=0.
 0006                   TCD(I)=0.
 0007                   TEF(I)=0.
 0008                   P1 (I)=0.
 0009                   P2 (I)=0.
 0010                25 CONTINUE
                C
                C       READ DATA
                C
```

FORTRAN IV G LEVEL 18 MAIN DATE = 70245 11/03/59

```
      READ(1,1) NF,NC,C1,C2,H
    1 FORMAT(2I5,3F10.4)
      NT=NF + NC
      WRITE(3,10) NF,NC,C1,C2,H,NT
   10 FORMAT('1',//,10X,'NF=',I3,5X,'NC=',I3,5X,'C1=',F10.4,5X,'C2=',
     &F10.4,5X,'H=',F10.4,5X,'NT=',I3)
C
C     DATA AT FREE BOUNDARY
C
      DELX=0.025
      DELY=DELX
      X=0.0
      PI=4.0*ATAN(1.0)
      AN1=1.0+146.0/180.0
      AN =1.0+140.0/180.0
      AN2=1.0+129.0/180.0
      H1=2.0*H
      THETA=0.0
      THETA1=0.0
      THETA2=0.0
      THETA1=THETA1*PI/180.0
      THETA2=THETA2*PI/180.0
C
C     COMPUTATION OF STRESSES AT FREE BOUNDARY
C
      PXX(1)=0.0
      PYY(1)=-AN*C1/H
      TAB(1)=AN1*C1*SIN(2.0*THETA1)/H1
      TCD(1)=AN2*C1*SIN(2.0*THETA2)/H1
      TEF(1)=0.0
      WRITE(3,20) PXX(1),PYY(1),TAB(1),TCD(1),X
   20 FORMAT(//,5X,5F21.8)
      I=1
C
C     READ PHOTOELASTIC DATA FOR INTERIOR POINTS
C
    5 READ(1,2) THETA1,THETA,THETA2,AN1,ANN1,AN,ANN,AN2,ANN2
    2 FORMAT(9F8.3)
C
C     COMPUTATIONS FOR POINTS WITHIN FACE SHEET
C
      I=I+1
      I1=I-1
```

```
FORTRAN IV G LEVEL  18                MAIN              DATE = 70245          11/03/59

0041          X=X+DELX
0042          THETA=THETA*PI/180.0
0043          THETA1=THETA1*PI/180.0
0044          THETA2=THETA2*PI/180.0
0045          IF(I1.GT.NF) GO TO 6
0046          TAB(I)=((AN1+ANN1/180.0)*C1*SIN(2.0*THETA1))/H1
0047          TCD(I)=((AN2+ANN2/180.0)*C1*SIN(2.0*THETA2))/H1
0048          TEF(I)=-((AN+ANN/180.0)*C1*SIN(2.0*THETA))/H1
0049          TABX=(TAB(I) + TAB(I1))/2.0
0050          TCDX=(TCD(I) + TCD(I1))/2.0
0051          DETXY=TABX-TCDX
0052          PXX(I)=PXX(I1)-DETXY*DELX/DELY
0053          PYY(I)=PXX(I) - (AN+ANN/180.0)*C1*COS(2.0*THETA)/H
        C
        C     MOHR'S CIRCLE FORMULA FOR CALCULATING PRINCIPAL STRESSES
        C
0054          AB=PXX(I) + PYY(I)
0055          CD=((AN+ANN/180.0)*C1)/H
0056          P1(I)=(AB+CD)/2.0
0057          P2(I)=(AB-CD)/2.0
0058          WRITE(3,30) I,P1(I),P2(I),PXX(I),PYY(I)
0059       30 FORMAT(//,5X,I3,4F21.8)
0060          GO TO 5
0061        6 CF=5.2
        C
        C     COMPUTATIONS FOR POINTS WITHIN CORE MATERIAL
        C
0062          AC=(AN+ANN)/CF
0063          AC1=(AN1+ANN1)/CF
0064          AC2=(AN2+ANN2)/CF
0065          TAB(I)=AC1*C2*SIN(2.0*THETA1)/H1
0066          TCD(I)=AC2*C2*SIN(2.0*THETA2)/H1
0067          TEF(I)=-AC*C2*SIN(2.0*THETA)/H1
0068          TCDX=(TCD(I) + TCD(I1))/2.0
0069          TABX=(TAB(I) + TAB(I1))/2.0
0070          DETXY=TABX-TCDX
0071          PXX(I)=PXX(I1)-DETXY*DELX/DELY
0072          PYY(I)=PXX(I) - AC*C2*COS(2.0*THETA)/H
        C
        C     MOHR'S CIRCLE FORMULA FOR CALCULATING PRINCIPAL STRESSES
        C
0073          AB=PXX(I) + PYY(I)
0074          CD=AC*C2/H
```

```
FORTRAN IV G LEVEL  18                MAIN              DATE = 70245        11/04/07
              C     ---------------------------------------------------------------
              C
              C     FINITE ELEMENT ANALYSIS OF SANDWICH CANTILEVER BEAM
              C
              C     ---------------------------------------------------------------
              C
              C
              C
              C     EF      - YOUNGS MODULUS OF FACE SHEET MATERIAL
              C     EC      - YOUNGS MODULUS OF CORE MATERIAL
              C     ANU     - POISSON'S RATIO OF CORE/FACE MATERIAL
              C     F       - THICKNESS OF FACE SHEETS
              C     H       - THICKNESS OF CORE
              C     AL      - LENGTH OF BEAM
              C     ALFA    - LENGTH OF AN ELEMENT OF BEAM
              C     NE      - NUMBER OF ELEMENTS
              C     NDF     - NUMBER OF DEGREES OF FREEDOM/NODE
              C     T       - TRANSFORMATION MATRIX
              C     TT      - TRANSPOSE OF INVERSE TRANSFORMATION MATRIX
              C     SM      - ELEMENT STIFFNESS MATRIX
              C     KODE    - CODE FOR APPLICATION OF BOUNDARY CONDITIONS
              C     V       - LOAD VECTOR FOR AN ELEMENT
              C     A       - OVERALL STIFFNESS MATRIX OF BEAM
              C     VL      - OVERALL LOAD VECTOR OF BEAM
              C     UA      - VECTOR OF AXIAL DISPLACEMENTS AT NODES
              C     UX      - VECTOR OF AXIAL STRAINS AT NODES
              C     W       - VECTOR OF TRANSVERSE NODAL DISPLACEMENTS
              C     WX      - VECTOR OF NODAL SLOPES
              C     WXX     - VECTOR OF NODAL CURVATURES
              C
              C
0001                IMPLICIT REAL *8(A-H,O-Z)
0002                DIMENSION T(10,10),TT(10,10),TB(10,10),SK(10,10),SM(10,10),M(10),
                   &N(10),V(10),U(10),UV(10),KODE(165,5),
                   &UA(33) ,UX(33),W(33),WX(33),WXX(33),
                   &A(165,165),VL(165),WW(165)
              C
              C     READ DATA ON NUMBER OF ELEMENTS, DEGREES OF FREEDOM PER NODE,
              C     NUMBER OF NODES PER ELEMENT AND LOADING MODE
              C
0003                READ(1,10) NDF,NE,NNE,LMODE
0004             10 FORMAT(4I5)
              C
              C     READ MATERIAL PROPERTIES, DIMENSIONS OF BEAM
```

```
FORTRAN IV G LEVEL  18                    MAIN                DATE = 70245          11/04/07          PA

                C
 0005                 READ(1,20) EF,EC,H,F,BB,ANU,AL
 0006              20 FORMAT(7F11.4)
 0007              21 WRITE(3,110) EF,EC,ANU,F,H,AL,LMODE
 0008             110 FORMAT('1', 9X,'YOUNGS MODULUS OF FACE MATERIAL        =',F15.4,//,
                     &          10X,'YOUNGS MODULUS OF CORE MATERIAL        =',F15.4,//,
                     &10X,'POISSONS RATIO FOR CORE=',F7.4,//,10X,'FACE THICKNESS=',F7.4,
                     &//,10X,'CORE THICKNESS=',F7.4,//,10X,'BEAM LENGTH=',F7.4 ,//,10X,
                     &'LOADING MODE=',I2)
                C
                C     CALCULATION OF ELEMENT STIFFNESS MATRIX SIZE(NN),TOTAL NODES(NNT)
                C     & OVERALL STIFFNESS MATRIX SIZE(M1)
                C
 0009                 NN=NDF*NNE
 0010                 NNT=NE+1
 0011                 M1=NDF*NNT
                C
                C     CLEAR ARRAYS
                C
 0012                 DO 30 I=1,10
 0013                 M(I)=0
 0014                 N(I)=0
 0015                 V(I)=0.0
 0016                 U (I)=0.0
 0017                 UV(I)=0.0
 0018                 DO 30 J=1,10
 0019                 TB(I,J)=0.0
 0020                 SK(I,J)=0.0
 0021                 SM(I,J)=0.0
 0022              30 CONTINUE
 0023                 DO 120 I=1,M1
 0024                 VL(I)=0.0D0
 0025                 DO 120 J=1,M1
 0026                 A(I,J)=0.0D0
 0027             120 CONTINUE
 0028                 DO 210 I=1,NNT
 0029                 W  (I)=0.0
 0030                 WX (I)=0.0
 0031                 WXX(I)=0.0
 0032                 UA (I)=0.0
 0033                 UX (I)=0.0
 0034             210 CONTINUE
 0035                 ALFA=AL/NE
```

```
FORTRAN IV G LEVEL  18                    MAIN                DATE = 70245          11/04/07        P

 0036           HBSQ=(H+F)**2                                                                 00000870
 0037           HF=H+F                                                                        00000880
 0038           ETA=EC/EF                                                                     00000890
 0039           RATIO=H/F                                                                     00000900
 0040           HD=H+ 2.0*F                                                                   00000910
 0041           AL BY D=AL/HD                                                                 00000920
 0042           F BY H=F/HD                                                                   00000930
 0043           GCBYEF=ETA/(2.0*(1.0+ANU))                                                    00000940
 0044           WRITE(3,22) GCBYEF,AL BY D,F BY H                                             00000950
 0045        22 FORMAT(//,9X,'GC/EF=',F15.10,//,10X,'L/D=',F20.8,//,10X,'F/H=',               00000960
               & F15.6)                                                                       00000970
          C                                                                                   00000980
          C     DEFINITION OF INDICES IN POLYNOMIALS FOR W AND U                              00000990
          C                                                                                   00001000
 0046           M(2)=1                                                                        00001010
 0047           M(3)=2                                                                        00001020
 0048           M(4)=3                                                                        00001030
 0049           M(5)=4                                                                        00001040
 0050           M(6)=5                                                                        00001050
 0051           N(8)=1                                                                        00001060
 0052           N(9)=2                                                                        00001070
 0053           N(10)=3                                                                       00001080
          C                                                                                   00001090
          C     TRANSFORMATION MATRIX ELEMENTS; ELEMENTS NOT SPECIFIED ARE ZERO               00001100
          C                                                                                   00001110
 0054           DO 31 I=1,10                                                                  00001120
 0055           DO 31 J=1,10                                                                  00001130
 0056           T (I,J)=0.0                                                                   00001140
 0057           TT(I,J)=0.0                                                                   00001150
 0058        31 CONTINUE                                                                      00001160
 0059           T( 1, 1)=1.0                                                                  00001170
 0060           T( 2, 2)=1.0                                                                  00001180
 0061           T( 3, 3)=2.0                                                                  00001190
 0062           T( 4, 7)=1.0                                                                  00001200
 0063           T( 5, 8)=1.0                                                                  00001210
 0064           T( 6, 1)=1.0                                                                  00001220
 0065           T( 6, 2)=ALFA                                                                 00001230
 0066           T( 6, 3)=ALFA**2                                                              00001240
 0067           T( 6, 4)=ALFA**3                                                              00001250
 0068           T( 6, 5)=ALFA**4                                                              00001260
 0069           T( 6, 6)=ALFA**5                                                              00001270
 0070           T( 7, 2)=1.0                                                                  00001280
 0071           T( 7, 3)=2.0*ALFA                                                             00001290
```

```
      T( 7, 4)=3.0*ALFA**2
      T( 7, 5)=4.0*ALFA**3
      T( 7, 6)=5.0*ALFA**4
      T( 8, 3)=2.0
      T( 8, 4)=6.0*ALFA
      T( 8, 5)=12.0*ALFA**2
      T( 8, 6)=20.0*ALFA**3
      T( 9, 7)=1.0
      T( 9, 8)=ALFA
      T( 9, 9)=ALFA**2
      T( 9,10)=ALFA**3
      T(10, 8)=1.0
      T(10, 9)=2.0*ALFA
      T(10,10)=3.0*ALFA**2
      WRITE(3,90)
   90 FORMAT(////)
      WRITE(3,60) ((T (I,J),J=1,10),I=1,10)
   60 FORMAT( 5(5X,E16.8))
C
C     INVERSION OF TRANSFORMATION MATRIX T
C
      CALL MATINV(T,10)
      WRITE(3,90)
      WRITE(3,60) ((T (I,J),J=1,10),I=1,10)
C
C     STORE INVERSE TRANSPOSE OF TRANSFORMATION MATRIX IN MATRIX TT
C
      DO 40 I=1,10
      DO 40 J=1,10
   40 TT(I,J)=T(J,I)
      WRITE(3,90)
      WRITE(3,60) ((TT(I,J),J=1,10),I=1,10)
C
C     DEVELOPMENT OF ELEMENT STIFFNESS MATRIX
C
C     INTEGRATION ROUTINE STARTS HERE
C
C
C     INTEGRAL  (WXX**2)
C
   61 DO 750 I=1,6
      DO 750 J=1,6
      MM=M(I)+M(J)-4
```

```
0101          MI=M(I)-1
0102          MJ=M(J)-1
0103          IF(MM.LT.0) GO TO 750
0104          IF(MI.LE.0.OR.MJ.LE.0) GO TO 750
0105          FACTR6=ALFA**(MM+1)/(MM+1)
0106          SK(I,J)=SK(I,J)+(F**2)*M(I)*M(J)*MI*MJ*FACTR6/12.0
0107      750 CONTINUE
0108          WRITE(3,60) ((SK(I,J),J=1,10),I=1,10)
        C
        C     INTEGRAL  (WX**2)
        C
0109          DO 751 I=1,6
0110          DO 751 J=1,6
0111          MF=M(I)+M(J)-2
0112          IF(MF.LT.0) GO TO 751
0113          FACTR3=ALFA** (MF+1)/(MF+1)
0114          SK(I,J)=SK(I,J)+ETA*RATIO*M(I)*M(J)*FACTR3/(4.0*(1.0+ANU))
0115      751 CONTINUE
0116          WRITE(3,60) ((SK(I,J),J=1,10),I=1,10)
        C
        C     INTEGRAL  (UX**2)
        C
0117          DO 752 I=7,10
0118          DO 752 J=7,10
0119          NF=N(I)+N(J)-2
0120          IF(NF.LT.0) GO TO 752
0121          FACTR1=ALFA**(NF+1)/(NF+1)
0122          SK(I,J)=SK(I,J)+N(I)*N(J)*FACTR1
0123      752 CONTINUE
0124          WRITE(3,60) ((SK(I,J),J=1,10),I=1,10)
        C
        C     INTEGRAL  (U**2)
        C
0125          DO 753 I=7,10
0126          DO 753 J=7,10
0127          NJF=N(I)+N(J)
0128          FACTR2=ALFA**(NJF+1)/(NJF+1)
0129          SK(I,J)=SK(I,J)+ETA*RATIO*FACTR2/(HBSQ*(1.0+ANU))
0130      753 CONTINUE
0131          WRITE(3,60) ((SK(I,J),J=1,10),I=1,10)
        C
        C     INTEGRAL  (UWX)
        C
```

```
0132            DO 754 I=1,6
0133            DO 754 J=7,10
0134            MFN=M(I)+N(J)-1
0135            IF(MFN.LT.0) GO TO 754
0136            FACTR4=ALFA**(MFN+1)/(MFN+1)
0137            SK(I,J)=SK(I,J)+ETA*RATIO*M(I)*FACTR4/(2.0*HF*(1.0+ANU))
0138        754 CONTINUE
          C
0139            WRITE(3,60) ((SK(I,J),J=1,10),I=1,10)
0140            DO 755 I=7,10
0141            DO 755 J=1,6
0142            MNF=M(J)+N(I)-1
0143            IF(MNF.LT.0) GO TO 755
0144            FACTR5=ALFA**(MNF+1)/(MNF+1)
0145            WRITE(3,756) I,J,MNF,FACTR5
0146        756 FORMAT(//,5X,3I5,5X,F15.8)
0147            SK(I,J)=SK(I,J)+ETA*RATIO*M(J)*FACTR5/(2.0*HF*(1.0+ANU))
0148        755 CONTINUE
          C
0149            WRITE(3,90)
0150            WRITE(3,60) ((SK(I,J),J=1,10),I=1,10)
          C
          C     MATRIX  SK(I,J)
          C
0151            DO 70 I=1,10
0152            DO 70 J=1,10
0153         70 SK(I,J)=    EF*BB*F*SK(I,J)
0154            WRITE(3,90)
0155            WRITE(3,60) ((SK(I,J),J=1,10),I=1,10)
          C
          C     MATRIX  (T)-1* (SK)
          C
0156            CALL MATMUL(TT,SK,TB,10,10,10)
0157            WRITE(3,90)
0158            WRITE(3,60) ((TB(I,J),J=1,10),I=1,10)
          C
          C     MATRIX  (T)-1T * (SK) * (T)-1= ELEMENT STIFFNESS MATRIX
          C
0159            CALL MATMUL(TB,T,SM,10,10,10)
0160            WRITE(3,90)
0161            WRITE(3,100)
0162        100 FORMAT(45X,'ELEMENT STIFFNESS MATRIX')
0163            WRITE(3,90)
```

```
0164            WRITE(3,60)   ((SM(I,J),J=1,10),I=1,10)
          C
          C     CHECK FOR TYPE OF LOADING
          C
0165        431 IF(LMODE) 131,132,131
          C
          C     CONSISTENT LOAD VECTOR
          C
0166        131 DO 130 I=1,6
0167            MU=M(I)+1
0168            U(I)=-ALFA**MU/MU
0169        130 CONTINUE
0170            DO 140 I=1,10
0171            V(I)=0.0
0172            DO 140 J=1,10
0173            V(I)=V(I) + TT(I,J)*U(J)
0174        140 CONTINUE
0175            WRITE(3,90)
0176            WRITE(3,60) (V(I),I=1,10)
0177            GO TO 134
          C
          C     LUMPED LOADING (OPTIONAL)
          C
0178        132 DO 133 I=1,10,NDF
0179            V(I)=-ALFA*BB/2.0
0180        133 CONTINUE
0181            WRITE(3,89)
0182         89 FORMAT(//,45X,'LUMPED LOAD VECTOR')
0183            WRITE(3,90)
0184            WRITE(3,60) (V(I),I=1,10)
          C
          C
          C     CALL SETUP SUBROUTINE TO ASSEMBLE OVERALL STIFFNESS MATRIX
          C     AND OVERALL LOAD VECTOR
          C
          C
0185        134 DO 105 K=1,NE
0186            READ(1,101)I,J
0187        101 FORMAT(2I5)
0188            CALL SETUP(I,J,A,M1,SM,NN,VL,V ,NDF)
0189        105 CONTINUE
          C
          C     AXIAL LOADING
```

```
            C
0190        11111 JJ=0
0191              DO 765 I=4,M1,5
0192              VL(I)=-0.05*JJ*AL*V(1)/NE
0193              JJ=JJ + 1
0194          765 CONTINUE
0195              WRITE(3,90)
0196              WRITE(3,60) (VL(I),I=1,M1)
0197          200 FORMAT(//,5(2X,D16.8))
0198              DO 221 I=1,M1
0199              IF(DABS(VL(I)).LE.1.0 D-06)  VL(I)=0.0D0
0200              DO 221 J=1,M1
0201              IF( DABS(A(I,J)).LE.1.0 D-07)      A(I,J)=0.0D0
0202          221 CONTINUE
            C
            C     APPLICATION OF DISPLACEMENT BOUNDARY CONDITIONS
            C
            C
            C     IF KODE(I,J)=0 THE CORRESPONDING ROW AND COLUMN ARE REPLACED BY
            C     ZEROS AND UNITY ON THE DIAGONAL ELEMENT; ALSO THE CORRESPONDING
            C     ELEMENT IN LOAD VECTOR IS SET TO ZERO. THIS GIVES THE SET BOUNDARY
            C     CONDITIONS IN SOLUTION ALONG WITH OTHER UNKNOWNS
            C
0203              WRITE(3,137)
0204          137 FORMAT(//,5X,'BOUNDARY CONDITIONS')
0205           62 DO 102 I=1,NNT
0206              READ(1,201) NP,(KODE(NP,K),K=1,NDF)
0207              WRITE(3,201)NP,(KODE(NP,K),K=1,NDF)
0208          201 FORMAT(6I5)
0209              DO 102 J=1,NDF
0210              NODE=KODE(I,J)
0211              IF(NODE) 102,103,102
0212          103 NL=(NP-1)*NDF + J
0213              DO 104 L=1,M1
0214              A(L,NL)=0.0D0
0215              A(NL,L)=0.0D0
0216          104 VL(NL)=0.0D0
0217              A(NL,NL)=1.0D0
0218          102 CONTINUE
            C
            C     INVERT OVERALL STIFFNESS MATRIX  A
            C
0219              CALL MATINV(A,M1)
```

```
FORTRAN IV G LEVEL  18                MAIN              DATE = 70245          11/04/07          PA
                C
                C     PREMULTIPLY LOAD VECTOR BY INVERSE OF OVERALL STIFFNESS
                C     THIS GIVES GENERALISED DISPLACEMENT VECTOR
                C
  0220                DO 240 I=1,M1
  0221                WW(I)=0.0D0
  0222                DO 240 J=1,M1
  0223            240 WW(I)=WW(I)+A(I,J)*VL(J)
                C
                C     SEPERATE THE GENERALISED DISPLACEMENT VECTOR TO GET TRANSVERSE
                C     DISPLACEMENT, SLOPE, CURVATURL, AXIAL DEFORMATION AND AXIAL STRAIN
                C
  0224                J=1
  0225                DO 160 I=1,M1,5
  0226                W(J)=WW(I)/HD
  0227                WX (J)=WW(I+1)
  0228                WXX(J)=WW(I+2)*HD
  0229                UA(J)=WW(I+3)/HD
  0230                UX (J)=WW(I+4)
  0231                J=J+1
  0232            160 CONTINUE
                C
                C     PRINT RESULTS
                C
  0233                WRITE(3,180)
  0234            180 FORMAT('1',//,16X,'STEP',17X,'W/H',17X,'WX',17X,'H*WXX',17X,'UA/H'
                    & ,18X,'UX')
  0235                WRITE(3,90)
  0236                DO 222 I=1,NNT
  0237                STEP=(I-1)*ALFA/AL
  0238                WRITE(3,170) I,STEP,W(I),WX(I),WXX(I),UA(I),UX(I)
  0239            170 FORMAT(//,5X,'NODE (',I2,')',F10.5,5(5X,D16.8))
  0240            222 CONTINUE
  0241                RETURN
  0242                END
```

```
FORTRAN IV G LEVEL  18                    MAIN                 DATE = 70245            11/03/59                PA

 0075                P1(I)=(AB+CD)/2.0                                                          00001300
 0076                P2(I)=(AB-CD)/2.0                                                          00001310
 0077                WRITE(3,31) I,P1(I),P2(I),PXX(I),PYY(I),TEF(I)                             00001320
 0078             31 FORMAT(//,5X,I3,5F20.8)                                                    00001330
 0079                IF(I.LE.NT) GO TO 5                                                        00001340
 0080                RETURN                                                                     00001350
 0081                END                                                                        00001360
```

## VII REFERENCES


1. Cook, R.D., " On Certain Approximations in Sandwich Plate Analysis," Journal of Applied Mechanics, Transactions of the ASME, March, 1966

2. Dally, J.W., and Riley, W.F., " Experimental Stress Analysis," McGRAW-HILL Book Company Inc., New York, N.Y., 1965

3 Dietz, A.G.H., " Composite Engineering Laminates," THE MIT PRESS, Cambridge, Mass., February, 1969

4. Durelli, A.J., Lake, R.L., and Tsao, C.H., " Device for Applying Uniform Loading to Boundaries of Complicated Shape," Proc. of SESA, 11, (1), 1953

5. Fang, T.C., Forray, M.J., and Benedicto, R.L., " Deflections and Stresses of a Clamped Rectangular Sandwich Beam," Journal of the Aerospace Sciences," November, 1962

6. Frocht, M.M., " Photoelasticity," Vols. 1 and 2, John Wiley and Sons Inc., New York, N.Y., 1967

7. Heller, R.A., " Interlaminar Shear Stresses in Sandwich Beams," Experimental Mechanics, September, 1969

8. Hoff, N.J., and Mautner, S.E., " Bending and Buckling of Sandwich Beams," Journal of the Aeronautical Sciences," December, 1948

9. Holand Ivar, and Bell Kolbein, " Finite Element Methods in Stress Analysis," TAPIR, The Technical University of Norway, Trondheim, Norway, 1969

10. Maple, J.A., " A Study of Finite Elements for the Analysis of Sandwich Plates," Ph.D Dissertation, Purdue University, Indiana, January,1969

11. Monforton, G.R., and Schmit Jr., L.A., " Finite Element Analysis of Sandwich Plates and Cylindrical Shells with Laminated Faces," Paper presented at the Second Conference on Matrix Methods in Structural Mechanics, Wright Patterson Air Force Base, Ohio, October 15 - 17, 1968

12. Plantema, F.J., " Sandwich Construction," John Wiley and Sons Inc., New York, N.Y., 1966

13. Raville, M.E., and Kimel, W.R., " On Small Deflection Theory for Sandwich Construction," Special Report No.2, Kansas Engineering Experiment Station, Kansas State College Bulletin, Vol. 43, No. 2, January 15, 1959

14. Reissner, Eric., " Finite Deflections of Elastic Sandwich Plates," Journal of the Aerospace Sciences," Vol. 15, July, 1948

15. Timoshenko, S., and Goodier, J.N., " Theory of Elasticity," McGRAW-HILL Book Company Inc., New York, N.Y., 1951

16. Yu, Yi-Yuan., " Flexural Vibrations of Elastic Sandwich Plates," Journal of the Aerospace Sciences, April, 1960

17. Zienkiewicz, O.C., and Cheung, Y.K., " The Finite Element Method in Structural and Continuum Mechanics," McGRAW-HILL Publishing Company Limited, London, England, 1967

18. Zienkiewicz, O.C., and Holister, G.S., " Stress Analysis," John Wiley and Sons Ltd., London, England, 1965